



**Aalto University**  
**School of Chemical**  
**Technology**

Marianne Joutti

## **Corrosion sensors for measuring industrial electronics lifetime**

Thesis submitted for examination for the degree of Master of  
Science in Technology.

Espoo 19.02.2014

Thesis supervisor: Professor Sami Franssila

Thesis instructor: Mikko Kohvakka, PhD and Mika Niemi,  
MSc.Tech

AALTO UNIVERSITY SCHOOLS OF TECHNOLOGY PO Box 12100, FI-00076 AALTO <a href="http://www.aalto.fi">http://www.aalto.fi</a>		ABSTRACT OF THE MASTER'S THESIS	
Author: Marianne Joutti			
Title: Corrosion sensors for measuring industrial electronics lifetime			
School: School of Chemical Technology			
Department: Applied Materials Science			
Professorship: Microtechnology		Code: MT 301-3	
Supervisor: Professor Sami Franssila  Instructor(s): Mikko Kohvakka, PhD and Mika Niemi, MSc.Tech			
<p>The purpose of this Master's Thesis was to find and test a sensor for Printer Circuit Board (PCB) corrosion monitoring and life cycle estimations. Commercial options and sensor structures presented in literature were inspected, but none of them could meet the demands for low price and spacing demands. Therefore, a novel corrosiometer was needed to be designed and tested.</p> <p>The corrosiometer presented in this Master's Thesis can be manufactured by same processes and materials as the PCB itself. Therefore, it does not raise manufacturing costs and it has the same production quality as the PCB itself. This sensor was tested in an artificial corrosion test called "GR-63-Core".</p> <p>This corrosiometer measures resistance change inside sensor copper patterns. It consists of two copper trace patterns, one of which measures insulation resistance of a PCB and the other measures the aging of copper traces. Four material combinations were tested: bare copper, immersion tin, solder resist and conformal coating coated copper traces. This sensor is meant to be used as a pair, in which the other sensor is made of corroding material and the other has been coated with corrosion preventive coating, and it works as reference sensor. Together with these patterns also typical PCB components were inserted in the sensor plate to simulate corrosion aging on PCB. These components were plated through holes, quad flat packages and resistors in serial of parallel connection patterns.</p> <p>The results of experimental tests pointed out, that corrosiometer presented in this Master's Thesis works. It can be used both for life-cycle analysis and condition monitoring of PCB. The best material combinations for corroding sensor was found to be bare copper and for reference sensor solder resist or conformal coated sensor.</p>			
Date: 19.02.2014		Language: English	
Number of pages: 55			
Keywords: PCB, corrosion of electronics, GR-63-Core, corrosiometer			

AALTO-YLIOPISTO TEKNIIKAN KORKEAKOULUT PL 12100, 00076 Aalto <a href="http://www.aalto.fi">http://www.aalto.fi</a>		DIPLOMITYÖN TIIVISTELMÄ	
Tekijä: Marianne Joutti			
Työn nimi: Korroosioanturi teollisuuselektroniikan eliniän määrittämiseen			
Korkeakoulu: Kemiantekniikan korkeakoulu			
Laitos: Materiaalitekniikan laitos			
Professuuri: Mikroteknologia		Koodi: MT3001	
Työn valvoja: Professori Sami Franssila			
Työn ohjaaja(t): Mikko Kohvakka, TkT and Mika Niemi, DI			
<p>Tämän diplomityön tarkoituksena oli löytää ja testata korroosioanturi piirikortin kunnonvalvontaan ja eliniänseurantaan. Kaupallisia ja kirjallisuudesta löytyviä anturimalleja tutkittiin, mutta mikään näistä vaihtoehdoista ei täyttänyt anturin alhaista tilavaatimusta ja riittävän matalaa hintaa. Tämän takia uusi anturi piti suunnitella ja testata.</p> <p>Tässä diplomityössä esitelty anturi voidaan valmistaa samoilla materiaaleilla ja menetelmillä kuin itse piirikortti. Täten se ei nosta valmistuskustannuksia ja sillä on sama tuotantolaatu kuin piirikortilla. Tämä anturi testattiin laboratoriossa tehdyllä korroosiotestillä, joka noudatti standardia "GR-63-Core". Tämä anturi mittaa resistanssin muutosta anturiin kuuluvilla kuparivedoilla. Anturi koostuu kahdesta erillisestä kuparivetokuvioista, joista toinen mittaa johdin- ja toinen eristysresistanssia. Anturin materiaaliveikotoina käytettiin paljasta kuparia sekä tinalla, juotteenestopinnoitteella tai lakalla päällystettyä kuparia. Tätä anturia on tarkoitus käyttää pareittain siten, että toinen antureista on valmistettu korrodoituvasta materiaalista ja toinen kuvio toimii samanaikaisesti referenssianturina. Tämä referenssianturi on päällystetty korroosion estävällä pinnoitteella. Näiden anturi kuvioiden lisäksi testikortille lisättiin elektronia komponentteja simuloimaan piirikortin komponenttien ikääntymistä.</p> <p>Tässä diplomityössä esitettyjen tulosten mukaan testattava anturi toimii ja se sopii sekä elinikämmäärityksiin että piirikortin kunnonvalvontaan. Parhaiten korrodoituvan anturin materiaali sopii testitulosten mukaan paljas kupari ja referenssianturille taas juotteenestopinnoitettu tai lakattu kupari.</p>			
Päivämäärä: 19.02.2014		Kieli: Englanti	
		Sivumäärä: 55	
Avainsanat: piirikortti, elektroniikan korroosio, GR-63-Core, korroosioanturi			

## Foreword

*The purpose of this Master's Thesis was done in order to design and evaluate a structure for corrosion sensor for Printed Circuit Board (PCB) corrosion monitoring. This sensor could give better understanding about corrosion aging of PCB, which could make it easier to take corrosion environment better into account during designing stage in demanding use environments with high temperature, humidity and in presence of corrosive agents. This Master's Thesis shall also describe theoretical aspects of corrosion phenomena on PCB and how corrosion environments can be categorized and corrosion rate inspected in laboratory tests.*

*I would like to thank Mikko Kohvakka and Mika Niemi, the instructors of this thesis, and whole ABB Oy Drives Technology department, for the support and opportunities given in this Master's Thesis. I would also like to thank Professor Sami Franssila and Professor Vesa Vuorinen and his research group for their contribution for this project.*

*Espoo 20.2.2014*

*Marianne Joutti*

## Index

Foreword .....	3
Index.....	4
Symbol unit definition .....	6
Abbreviations .....	7
1 Introduction .....	8
1.1 Background .....	8
1.2 The Research motivation .....	9
1.3 The goal of this project.....	10
1.4 Borderlines and scope .....	10
1.5 Requirements.....	10
2 Corrosion.....	11
2.1 Definition of Corrosion .....	11
2.2 Corrosion mechanisms .....	11
2.2.1 Electrical corrosion .....	11
2.2.2 Migration of corrosion products.....	11
2.2.3 Galvanic corrosion .....	12
2.2.4 Other corrosion mechanisms.....	13
2.3 PCB materials vulnerable parts to corrosion .....	14
2.4 Corrosion environments, corrosive agents and corrosion standards .....	15
2.4.1 Humidity and temperature.....	16
2.4.2 The role of chemicals and conductive dust in corrosion.....	18
2.5 Corrosion environment standards.....	21
2.5.1 ISO 9223 .....	22
2.5.2 IEC 60721 .....	23
2.5.3 ANSI/ISA-S71.04 .....	24
2.5.4 Standard summary and target corrosivity class in laboratory tests .....	24
2.6 Standardized corrosion tests .....	27
3 Insulation and conductor resistance .....	29
3.1 Insulation resistance .....	29
3.2 Surface insulation resistance .....	30
3.3 Conductor resistance .....	30
4 Corrosion Sensors .....	31
4.1 Mass change methods.....	31
4.2 Coulometric methods .....	33
4.3 Quartz crystal microbalance .....	33
4.4 Electrical resistance sensors .....	34
4.4.1 Electrical resistance sensor structures.....	35
5 Experimental .....	40
5.1 Proposed new corrosiometer structure .....	40
5.2 Sample preparation and used material combinations .....	42
5.3 Choosing test standard.....	42
5.4 GR-63-CORE correspondence with use life and achieved resistance changes..	44
5.5 Test set-up and equipment.....	45
6 Results .....	49
6.1 Corrosion sensor resistance .....	49
6.1.1 Conductor resistance .....	49
6.1.2 Insulation resistances .....	52

6.2	Reference components .....	53
6.2.1	Plated through holes .....	53
6.2.1	Quad flat packages .....	54
6.2.2	Serial and parallel resistors .....	55
6.2.3	Other reference samples .....	57
6.3	Test corrosiveness on copper .....	58
6.4	Summary of results and comparison with Vahter's results .....	61
7	Conclusions .....	63
	References .....	64
	Appendix A. Corrosion rates and corrosion studies in tropical environments .....	66
	Appendix A References .....	67
	Appendix B. Sample numbers.....	68
	Appendix C. Reference result graphs for chapter 6.4 .....	69

## Symbol unit definition

A	[mm <sup>2</sup> ]	Area
CD	[m]	Corrosion Depth
f	[Hz]	Frequency
I	[A]	Current
L	[m]	Distance
m	[kg]	Mass
N		Frequency Constant
R <sub>C</sub>	[Ω]	Conductor Resistance
ΔR <sub>C</sub>	[Ω]	Conductor Resistance change during testing
RH	[%]	Relative humidity
R <sub>I</sub>	[Ω]	Insulation Resistance
R <sub>P</sub>	[Ω]	Surface Insulation Resistance (SIR)
s	[m]	Length
t	[μm]	Thickness
T	[°C]	Temperature in Celsius-degrees
U	[V]	Voltage
w	[m]	Width
τ <sub>1</sub> –τ <sub>6</sub>	[h]	Time of Wetness (TOW)
ρ <sub>PCB</sub>	[Ω*m]	PCB Resistivity
ρ	[Ω*m]	Resistivity
μ	[H/m]	Natural Permeability
σ	[1/ Ω*m]	Conductivity

## Abbreviations

AC	Alternating Current
ANSI/ISA-S.7104	Corrosion Standard published by ISA
DC	Direct Current
CFC	Chlorofluorocarbon
C1–C5	Corrosion classes according to ISO 9223
EDS	Energy Dispersive x-ray Microscopy
EMC	Electromagnetic Compatibility
ENIG	Electroless nickel immersion gold
FR-4	Glass-reinforced epoxy laminate sheet
GR-63-Core	Corrosion standard published by Telcordia
G1–GX	Corrosion classes according to ANSI/ISA-S.7104
HASL	Hot Air Solder Leveling
IEC	International Electrotechnical Commission
IEC 60721	Corrosion Standard published by IEC
ISA	International Society of Automation
ISO	International Organization for Standardization
ISO 9923	Corrosion standard published by ISO
ISO 10062	Corrosion Test published by ISO
LCD	Liquid Crystal Display
PCB	Printed Circuit Board
PCBA	Printed Circuit Board Assembly
ppb	Parts per billion
ppm	Parts per million
PTH	Plated Through Holes
QFP	Quad Flat Package
SEM	Scanning Electron Microscope
SIR	Surface Insulation Resistance
TOW	Time of Wetness
3C1–3C3	Corrosion classes according to ANSI/ISA-S.7104
85 °C/85 % RH	Corrosion test with 85 °C temperature and 85 % relative humidity
40 °C/90 %	Corrosion test with 40 °C temperature and 90 % relative humidity



# 1 Introduction

In this section the reliability of requirements and monitoring methods for frequency converters are reviewed.

## 1.1 Background

This thesis discusses the sensing of corrosion in electronics that controls electric motors in industrial applications. Most of these motors today use alternating current (AC) as input and their speed and torque are depended on the frequency and voltage of the AC input. The frequency of the alternating current of the grid is usually 50–60 Hz, and if motor needs to operate faster or slower, a drive is needed. There are two main types of drives: direct and with intermediate circuit. In direct drives the input alternating current is chopped into a wanted frequency and current output by utilizing semiconductor switches. (Niiranen 2000, P. 48–49)

The structure of a drive with an intermediate circuit is described in figure 1. The three-phase input current (with phases U1, V1 and W1) in the left corner is EMC- filtered and rectified into a direct current (DC) and converted back into alternating output current by an inverter. EMC-filtering is done to reduce the amount of interference signals from the drive to the grid. The intermediate circuit is situated between rectifier and inverter. It has big capacitors and a brake resistor to stabilize DC voltage. The brake chopper and braking resistor are used during motor braking when the deceleration energy is dissipated in the brake resistor. The voltage of the intermediate circuit is measured with a measuring unit which also monitors inverter voltages and currents directed into the motor. The measuring unit is connected to the control unit of the drive. This control unit consists of the control panel, I/O interfaces for external controlling units and motor peripherals. Based on results given by the measuring unit, the motor control unit adjusts the voltages and currents in the way that the motor operates in a desired way. The intermediate circuit also gives input voltage to the power supply of the drive which in turn distributes desired supply voltages to the control and measuring unit. (Kiiski 2012, P. 5).

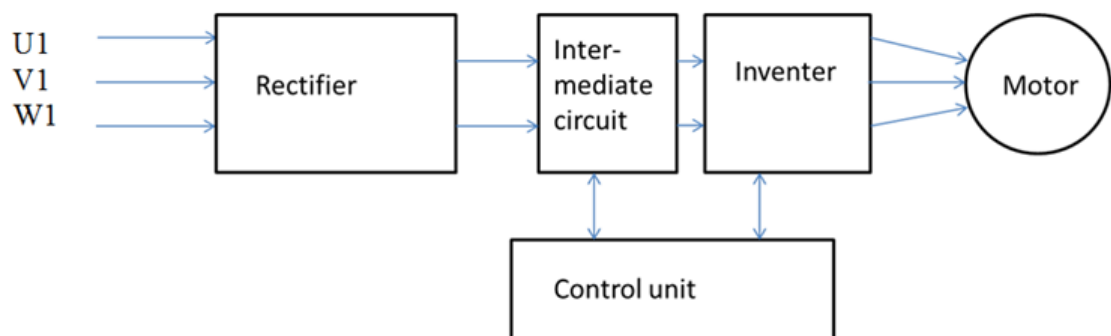


Figure 1. Structure of a drive with an intermediate circuit (Re-drawn after Niemi 2006, P. 9).

The aforesaid electronics is implemented in a Printed Circuit Board (PCB). The assembly of PCB and electronic components is called Printed Circuit Board Assembly (PCBA). In figure 2 some of these drives, with their plastic encapsulations, are shown. Although these drives are enclosed into closed plastic housings, many mechanical structures and therefore PCBAs are often open in order to get better cooling. Because of the open structure airborne gases, chemical compounds and pollution have a corrosive effect to the PCBA. This is especially true in highly polluted places such as in heavy industry or inside mines, in tropical atmosphere or seashore.



*Figure 2. Drives attached to a wall (Kiiski 2012, P. 4).*

## **1.2 The Research motivation**

The main motivation for this study was to develop a method that would predict and prevent occurring failures. Because drives are meant to be used for a long time (10–25 years), their robustness is imperative and it is important to receive a pre-warning of an occurring failure. It is also considered beneficial to gather knowledge, on PCBAs aging during their life time. This all would help designers to take the use environment better into account in designing stage and tailor the corrosion prevention measures accordingly. This life cycle knowledge could also make warranty handling easier as corrosiometer gives in-situ information in which kind of environment the drive has been used. Corrosiometer is a sensor, which measures corrosion rates or environmental factors causing corrosion

### **1.3 The goal of this project**

The purpose of this project and Master's Thesis was to design and evaluate a structure for a corrosiometer. It was also important to gather information about corrosion mechanisms and typical failure modes from literature and environmental testing. Additionally, there was a need for to study different corrosion mechanisms affecting the PCBA and related components and search for different corrosion sensors suitable for monitoring the corrosion rate of PCBA.

### **1.4 Borderlines and scope**

This work focuses solely on failures caused by corrosion on the PCBA and how to design a corrosion sensor or corrosiometer that can be used to warn operators or maintenance personnel about imminent failure before actual damage is caused to the system. However, sensor readout electronics was left outside the scope of this Master Thesis, as they will be handled in other projects. Environmental monitoring of drives during manufacturing, storage and transporting from ABB factory to customer was determined to be kept outside scope of this Master's Thesis because of difficulty achieving data from this period. Also mechanical loading such as vibration and thermo mechanical failures (creep/fatigue) were excluded due to their case sensitivity which both makes their simulation in a laboratory environment hard to plan and to carry out.

### **1.5 Requirements**

Operating ambient temperature range for PCB components used in industrial drives varies usually between approximately -40 – 85 °C and in some special cases -40–105 °C or -40 – 125 °C (ABB Oy 2013, a and b). The size demand of a sensor depends strongly on where it is installed but usually it should be less than 200 mm<sup>2</sup>. The sensor has to be easily integrated to the manufacturing processes of PCBA and be as cheap as possible (less than \$ 3 per piece).

Things to consider when planning the structure of a corrosiometer include:

- a component already on the market
- a component that could be developed in co-operation with a IC manufacturing partner
- a technology that could be integrated on a PCB
- a technology requiring no additional material, only taking advantage of elements of the bare PCB (copper wiring, solder alloy, solder resist, conformal coating)

To reach high cost effectiveness, the idea is to use as much as possible same materials and components which are already used in mass manufacture. This is also reasonable because their reliability behavior in usage conditions is relatively well known and ABB assembly process is more likely to be compatible with the developed sensor.

## 2 Corrosion

The prior knowledge of corrosion failures of PCBA focuses mostly on failure reports from the field and different corrosion tests done in laboratory. Corrosion itself is a natural physico-chemical phenomenon, in which materials try to revert to a more energetically favorable condition. In practice this means that processed materials, such as metals, try to change back to ores consisting of metal oxides, sulfides or other chemical compounds. (Aromaa 2005, P. 5). With other materials, such as polymers, ceramics or composite materials, degradation mechanism are not usually called corrosion but also in them environment slowly destroys them with the aid of temperature, moisture and mechanical stress which together brittles and destroys the chemical bonds inside these materials (Aromaa 2005, PP. 115–118).

In this chapter corrosion mechanisms and factors causing or accelerating corrosion are introduced followed by corrosion standards and corrosion tests.

### 2.1 Definition of Corrosion

Corrosion is a chemical reaction where less noble material is oxidizing and noble ions are reducing. Due to this reaction less noble materials are consumed away and noble ions are precipitated from the electrolyte. For corrosion to occur following conditions has to be present (Aromaa 2005, P. 24, Henriksen et al. 1991, PP. 19 - 24):

- Conductive electrolyte (water + pollutants)
- Corrosion pair (two or more materials with different electrochemical nobilities)
- Electrical connection between the corrosion pair

In addition, there are environmental factor which accelerate corrosion rate

- Halides, sulfides or ammonia which can destroy locally protective layer and therefore promote corrosion
- Humidity ( $RH > 50\%$ )
- Elevated temperature (for example  $> 40\text{ }^{\circ}\text{C}$ ).

### 2.2 Corrosion mechanisms

#### 2.2.1 Electrical corrosion

Electrical corrosion occurs where conductor materials with different electrochemical potentials are connected by an electrolyte or connector. Ions move from the nobler material toward the lower potential material and these moving ions therefore cause short circuits between these conductors. Even with small voltages high electrical fields are born when conductor distances are small. (Tolvanen 1996, P. 23).

#### 2.2.2 Migration of corrosion products

In some cases the corrosion products of copper and silver migrate to the surface of the PCB and form a thin conductive layer. This phenomenon is typical when silver plating is coated with a gold layer. Corrosion products of copper move to the top of both silver and gold plating. Gold is both an expensive and porous material and it is not suitable for demanding conditions and, due to its high price, it is rarely used in low-cost ABB drives (Tolvanen 1996, P. 24).

### 2.2.3 Galvanic corrosion

Galvanic corrosion occurs in situations where materials with different electrical potentials are connected to each other with a direct connection to each other (usually weld or electrolyte). The principle of galvanic corrosion is presented in figure 3, where the yellow presents the nobler and grey is the less noble material, which is corroded away while the noble material stays intact.

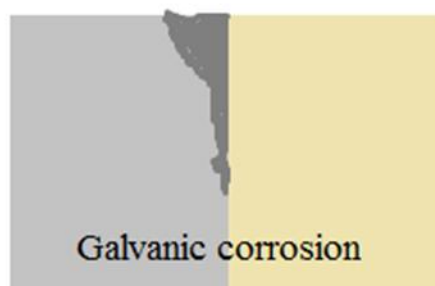


*Figure 3. Galvanic Corrosion in the border region between two materials with different electrical potentials (re-drawn after Aromaa 2005, P. 64).*

Tolvanen states (1996, P. 24), that potential difference or voltage between directly connected materials should not be over 0.25 V in weather susceptible conditions. If conductor area is well protected, the allowed maximum voltage is 0.50 V. In table 1 some most commonly used materials and their potentials are presented in seawater (temperature +25°C) with calomel electrode (SCE) as a counter electrode.

*Table 1. Electrical potentials of most common PCB materials (Tolvanen 1996, P. 24).*

Metal	Potential vs. SCE, (V)
Aluminium	-0.75
Silver-lead solder	-0.50
Tin solder	-0.48
Stainless steel	-0.20 – -0.45
Tin	-0.26
Nickel silver	-0.19
Copper	-0.18
Silver plating	+0.01

As can be seen in the table 1, the potential difference between copper and tin is merely 0.08 V. Because of this, tin is used as a protective coating for copper or steel. Its protection ability is based on its ability to form uniformly dense plating, which prevents impurities or humidity reaching the coated base metal. Therefore tin is a great choice as protective coating for copper because it stops copper from reacting with impurities in air. Other things affecting to the galvanic corrosion is the size ratio between cathode (noble metal) and anode areas (less noble metal areas). If the area of less-noble material is lower than the area of nobler material, it slows the corrosion rate and forming of corrosion products. Usually, corrosion products are forming on the top of less-noble material, close to the border area between the two different metals, while noble material stays intact (Aromaa 2005, PP. 97–98, 114).

#### 2.2.4 Other corrosion mechanisms

In this chapter other usual corrosion mechanisms are discussed. These mechanisms have some impact on PCBA corrosion but due their universal nature they are not described in detail here. Common corrosion is the most predictable corrosion form because the corrosion rate is almost same throughout the whole surface. Crevice, pitting and galvanic corrosion are local corrosion mechanisms, as they are caused by local impurities or material differences. In crevice and pitting corrosion, strong corrosive agents or mechanical wear-out or stress destroys the passive layer, which insulates the material from environment, and local corrosion starts. As the pit or crevice deepens, inside conditions become harsher, and corrosion rate increases. In figure 4 typical corrosion mechanisms are illustrated.

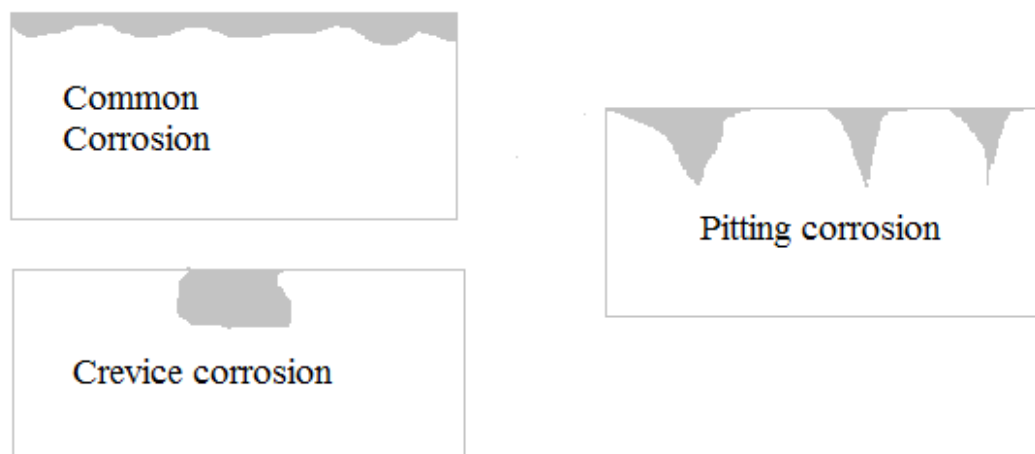


*Figure 4. Common corrosion mechanisms: common, pitting and crevice corrosion (Re-drawn after Aromaa 2007, P. 64).*

### 2.3 PCB materials vulnerable parts to corrosion

In table 2 typical materials for electronics are given. Copper is the most used material in whole electronics industry, and for example conducting traces are usually pure copper. Screws and conductors are often made of bronze and brass alloys. A typical structure of a connector's coating structure of is presented in figure 5. The base material is usually coated with a barrier layer, whose function is to protect the base material. It is also possible that copper tries to diffuse from the base material towards the surface of the connector. This copper diffusion can be stopped by protective nickel pre-layer plated before the actual immersion layer, which can be silver, platinum, gold or other precious metal. The surface plating gives the structure mechanical and chemical protection. Additional protection can be given with an optional solder resist and/or conformal coating. Both or these coatings are usually made of polymers. They are used in order to stop solder reaching unwanted areas (solder resist) or stop humidity and corrosive agents reaching materials below. Copper corrodes usually by common corrosion, but strong oxidizers such as chlorine and sulphur compounds can promote also local corrosion. When plated copper is used, the corrosion usually starts from local pores, where the protective oxide barrier has been destroyed and corrosion products diffuse to the top of copper. (Hienonen and Lahtinen, 2007, P. 158 and Aromaa 2007, PP. 111–112).

*Table 2. Materials for electronics (modified after Hienonen and Lahtinen, 2007, P. 158).*

Part	Materials
Cabinets, racks, springs and heat sinks	Aluminium, steel, brass, bronze, copper, zinc nickel and copper coatings
Printed Circuit Board	Copper, copper alloys, tin and gold coatings
Electrical contacts and groundings	Copper alloys, steel, aluminium, contact platings such as gold, palladium, silver-palladium, silver and tin
Connectors	Brass, beryllium-copper, phosphor-bronze, chromium stainless steel and contact platings
Switches and relays	Copper alloys, steels, chromium and stainless steel
Passive and semiconductor components and microcircuits	Gold, copper alloys, nickel as barrier layer, silver, aluminium, kovar (nickel-steel alloy) and wolfram

In PCBs used by ABB connection pads to components and connectors are typically coated with tin. Elsewhere, PCB surface is coated with solder resist. On top of PCB and components, uniform acrylic conformal coating is used as a final coating layer.

PCB parts which are most prone to corrosion (Tolvanen 1996, PP. 23–27)

- Electro plated silver, aluminum and copper parts
- Silver and copper contacts
- Solder materials (tin, silver and copper etc.)
- Corrosion (loss of material) mechanisms in bare PCBA materials, conductors, components and solder alloys

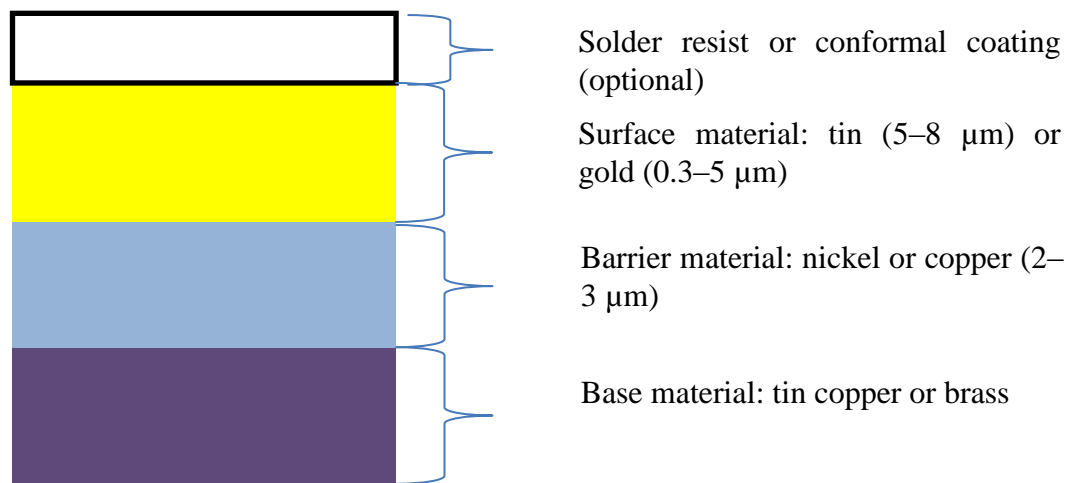


*Figure 5. Plated structure of a connector (re-drawn after Hienonen and Lahtinen, 2007, P. 135).*

Due to the multilayer structure used in PCBA, it would also be beneficial to inspect how a controlled corrosion test affects the corrosion of different coating combinations used in PCBAs made by ABB Oy. This test setup is described in detail later on.

## **2.4 Corrosion environments, corrosive agents and corrosion standards**

The most common factors causing problems with electronics are heat, vibration and humidity aided by dust and/or other pollution. Their contribution to the occurrence of electronics failures vary depending of the environment. An example from the relevant importance of each factor from aviation industry is given in figure 6. Corrosion is one the most important failure mode in electronics. Temperature, temperature fluctuation and humidity are root causes to different corrosion mechanisms and their severity due to thermodynamics and environmental parameters (humidity and pollution). All these factors can also accelerate corrosion rates and therefore cause increased failure rates in PCBAs used in the field. (Hienonen and Lahtinen 2007, P. 18).



Dust and vibration are not usually causing corrosion directly, but conductive dust (for example coal dust) can collect humidity from air and therefore can cause optimal conditions for chemical oxidation-reduction reactions, which are the root causes for corrosion. Vibration causes mechanical strain to PCB components and can therefore break component leads and solder junctions (Karppinen 2013, PP. 59–60).

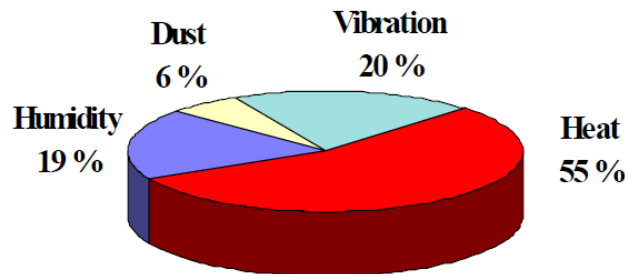


*Figure 6. Environmental factors contributing to failures of PCB in aviation industry: heat, vibration humidity and dust (Hienonen and Lahtinen, 2007 P. 18).*

The other acceleration factors contributing to PCBA corrosion problems are related to material properties (available corrosion pairs and their passivation capacity for passivation) and for example air pollutants such as  $\text{Cl}_2$ ,  $\text{H}_2\text{S}$ ,  $\text{SO}_2$  and  $\text{NO}_2$ .

#### **2.4.1 Humidity and temperature**

Corrosion in PCBA is predictable when environmental conditions allow condensation of humidity (RH near 100 %). On the other hand, corrosion is not likely to be a problem in conditions where relative air humidity is below 40 % and temperature lower than 40 °C. In these optimal conditions a majority of corrosion problems do not occur, or they are slow enough not to cause problems during the life cycle of the system. However, in practice these conditions are possible only in well ventilated indoor locations, as can be seen in figure 7, where statistics of typical temperature and air humidity for polar and temperate climates in different seasons are presented (Middle Europe, Canada and Northern parts of USA).

When the relative humidity exceeds 60 %, corrosion is still relatively slow, but at 70–90 % relative humidity, the corrosion rates grow significantly. As a rule of thumb, corrosion rates typically double for a rise of ten Celsius-degrees. It is also important to remember that corrosion can be a problem also when temperature changes rapidly. A good example of this is morning mist, when the surfaces of electronic components are cool, but because air is warming up fast and absolute humidity (the amount of water in air in  $\text{g/m}^3$ ) is rising, moisture starts to condensate on top of or inside electrical components if necessary ventilation is not taken properly care of. (Hienonen and Lahtinen 2007, PP. 14–15, 47–51)

As can be seen in the figure 7, relative humidity stays always over 60 % and during winter time (November to October) it exceeds 90 %. Air humidity is even higher in tropic areas and near seaside relative (Hienonen and Lahtinen 2007, P. 15).

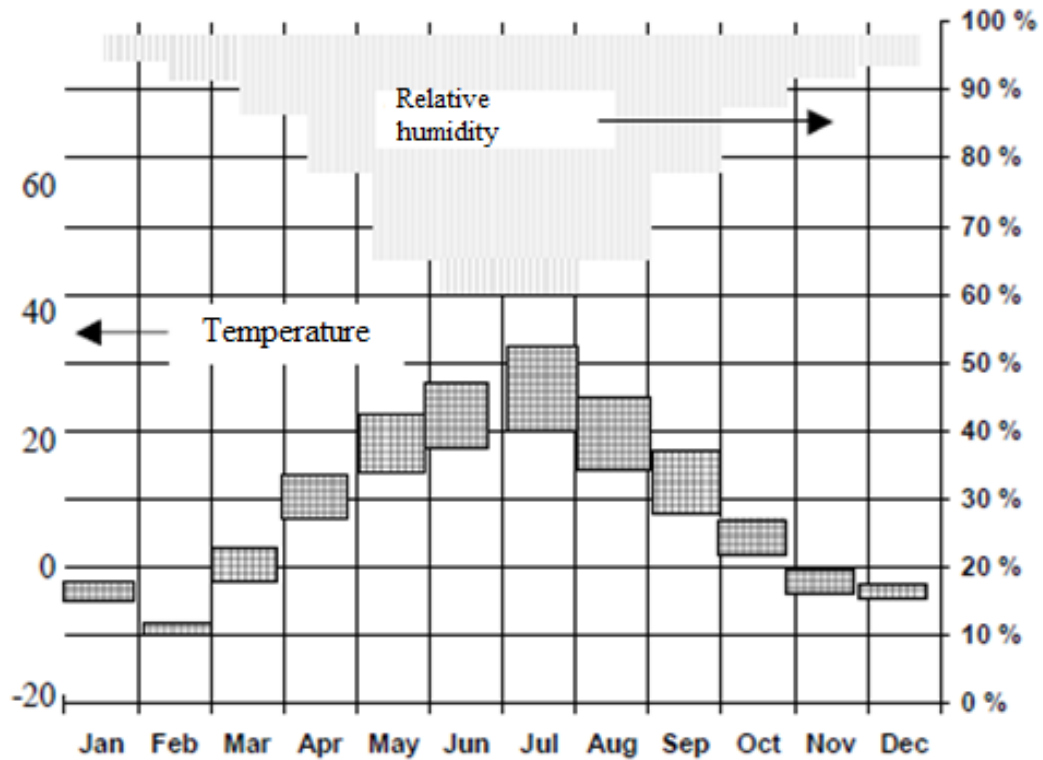


Figure 7. Typical corrosion environment (relative air humidity and temperature) outside in polar and temperate climates in different seasons (Middle Europe, Canada and Northern parts of USA) (Hienonen and Lahtinen 2007, P. 15).

Inside a drive the temperature is usually kept 10–20 °C above the surrounding environment to prevent condensation of humidity to the surfaces of PCB components (Kiiski 2012, P. 29). In figure 8 typical curves for tropical dry (desert) and humid tropical areas are presented. Tropical dry curve is marked with blue and humid curve with red color. For example, if air temperature is approximately 30 °C and RH 65 % in tropical temperature (blue curve), then drive's internal temperature is 50 °C and relative humidity of air is approximately 25 %.

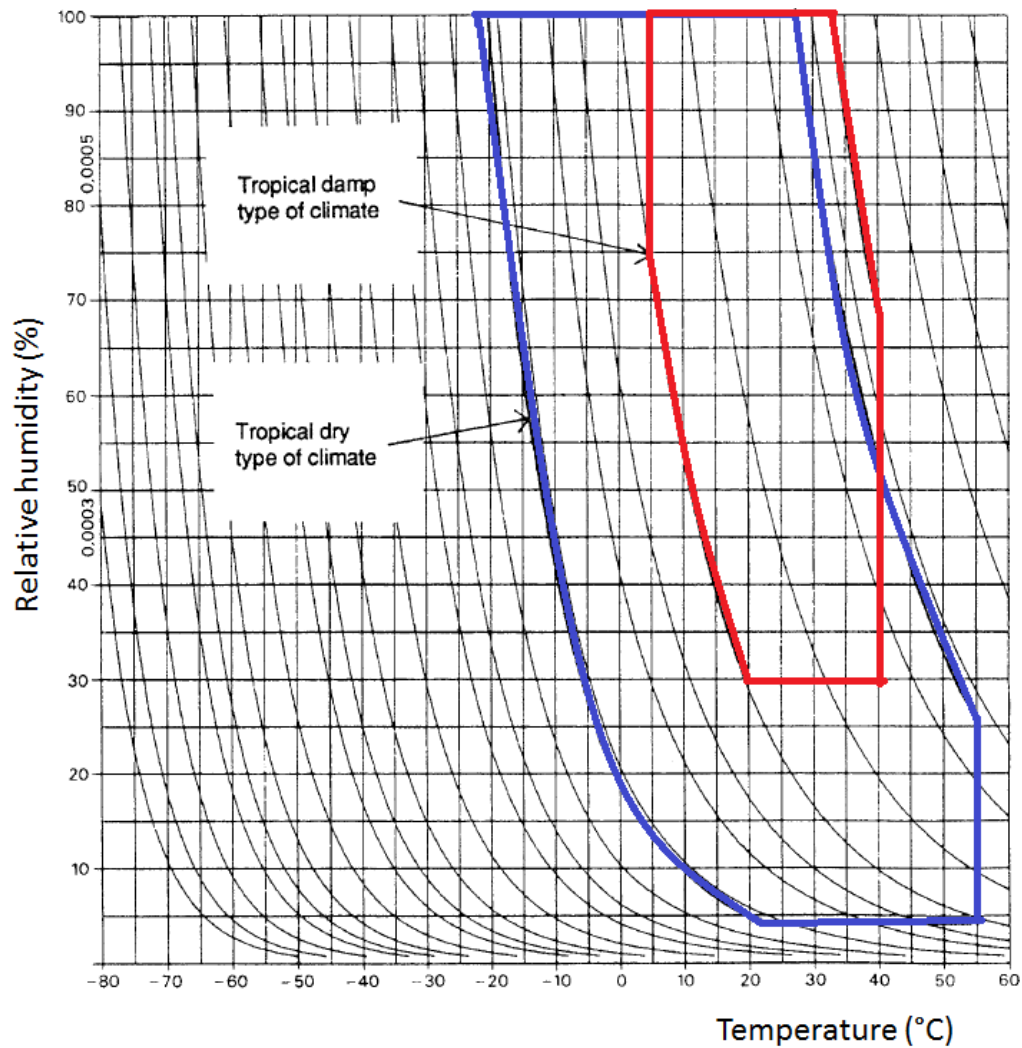


Figure 8. Temperature-humidity curves in tropical areas. Blue curve presents typical tropical dry and red curve tropical damp type of climate (IEC 60721-3-3 1994, P. 101.).

#### 2.4.2 The role of chemicals and conductive dust in corrosion

In harsh environments, with high humidity and temperature combined and corrosive agents accelerating normal corrosion mechanisms, drives can be subjected to demanding conditions. Most often corrosion standards (for example ISO 9223 and IEC 60721-3-3) state that chlorine, sulfur dioxide, nitrogen oxide and hydrogen sulphite are mentioned to be the most corrosive agents. Some of these chemicals are also present in semiconductor manufacturing processes, such as soldering fluxes, which contain chlorine. Next these most important corrosive gases are described in detail.

#### **2.4.2.1 Chlorine (Cl<sub>2</sub>)**

Chlorine is a strong oxidizer and therefore corrosion catalyst, which can cause for local destruction of the passive oxide layer. It is known to be most harmful to ferrous metals and less to copper and zinc alloys (Revie 2000, P. 312). Main sources for chlorine are sea water, heavy industry, such as paper factories, and desert salt in areas, where the ground is ancient seabed (ISO 9223 2012). A notable source for chlorine for PCB is traditional manufacturing processes, such as etching or after soldering when CFC-based (chlorofluorocarbons) cleaning agents were used. Today, the use of CFC-detergents is forbidden and other manufacturing processes which for example do not include washing are used instead. (Tolvanen 1996, P. 35, 39)

#### **2.4.2.2 Sulphur dioxide (SO<sub>2</sub>)**

Sulphur dioxide is an acid rain component which reacts with water and forms sulphur acid H<sub>2</sub>SO<sub>4</sub>. It is a diminishing, but still important source of corrosion especially in the developing countries (Revie 2000, P. 311). Main sources for sulphur dioxide and other sulphur compounds are heavy industry and volcanic activity (ISO 9223 2012).

#### **2.4.2.3 Hydrogen sulfide (H<sub>2</sub>S)**

Hydrogen sulfide is a very corrosive to most metals/alloys and the corrosive effects of gaseous chlorine and hydrogen chloride in the presence of moisture tend to be stronger than those of chloride compounds. Both SO<sub>2</sub> and S<sub>2</sub>H are harmful to silver and copper alloys (Henriksen et al. 1991, PP. 41–42).

#### **2.4.2.4 Nitrogen oxides (NO<sub>x</sub>), Ozone (O<sub>3</sub>) and other chemicals**

Nitrogen oxides (NO<sub>2</sub> most often mentioned), ammonia and ozone are important corrosion agents, as they can form nitric acid (HNO<sub>3</sub>), and are able to accelerate atmospheric corrosion rate in copper several times, when SO<sub>2</sub> is present. Nitrogen compounds, in the form of NO<sub>x</sub>, also tend to accelerate atmospheric attack. The NO<sub>x</sub> compounds are formed largely from combustion (for example traffic) processes and have been reported to have increased in relation to SO<sub>2</sub> levels. However, measured deposition rates of these nitrogen compounds have been significantly lower than those of SO<sub>2</sub>, which probably accounts for the generally lower importance assigned to these. Generally researchers think that at ppm range nitrogen oxides have a very slight effect on corrosion of copper. (Revie 2008, P. 303-304 and ISO 9223 2012). Ozone itself without nitrogen oxides is not so significant, because it is not stable at ground level. Also carbon dioxide (CO<sub>2</sub>), oxygen (O<sub>2</sub>) and hydrogen peroxide (H<sub>2</sub>O<sub>2</sub>) are thought to have some effect on corrosion of metals, but they are not mentioned in standards (Revie 2000, PP. 309–311).

As a summary the following table 3 highlights common pollutants in industrial environments. As can be seen, together with inorganic chemical compounds, also some organic compounds (wood fibers and aldehydes, carbon monoxide and other hydrocarbons) are mentioned as sources for pollution. However; inorganic corrosive gases presented in this chapter are commonly thought to contribute more to corrosion of electronics. Bromides are not mentioned in corrosion prevention standards or guide books either.

Table 3. Common pollution types in five industrial environments (Tolvanen 1996, P. 20).

Processing environment	Pollution
Energy	SO <sub>2</sub> , C, CO, NO <sub>x</sub> , hydrocarbons and other organic compounds
Paper and pulp industry	Cl <sub>2</sub> , SO <sub>2</sub> , H <sub>2</sub> S, CO, wood fibers, dust
Wastewater treatment	NH <sub>3</sub> , H <sub>2</sub> S, H <sub>2</sub> , S, CO and aldehydes
Traffic	SO <sub>2</sub> , SO <sub>3</sub> , HCl, HBr, NO <sub>x</sub> , CO, hydrocarbons and other organic compounds
Harbours	NaCl, chlorides

#### 2.4.2.5 Conductive dust

Dry dust itself is not usually a big corrosion risk for metals or electronics although in humid atmosphere dust is very good humidity collector. Humid dust combined with or including corrosive chemicals can cause perfect conditions for local corrosion. Additionally, conductive dust together with humidity can cause short circuit. Desert sand can also cause mechanical damage and local corrosion if sand includes sea salt. In figure 9 the effect of different kinds of dust samples around the world, combined with relative humidity to the presence of leakage currents, are presented.

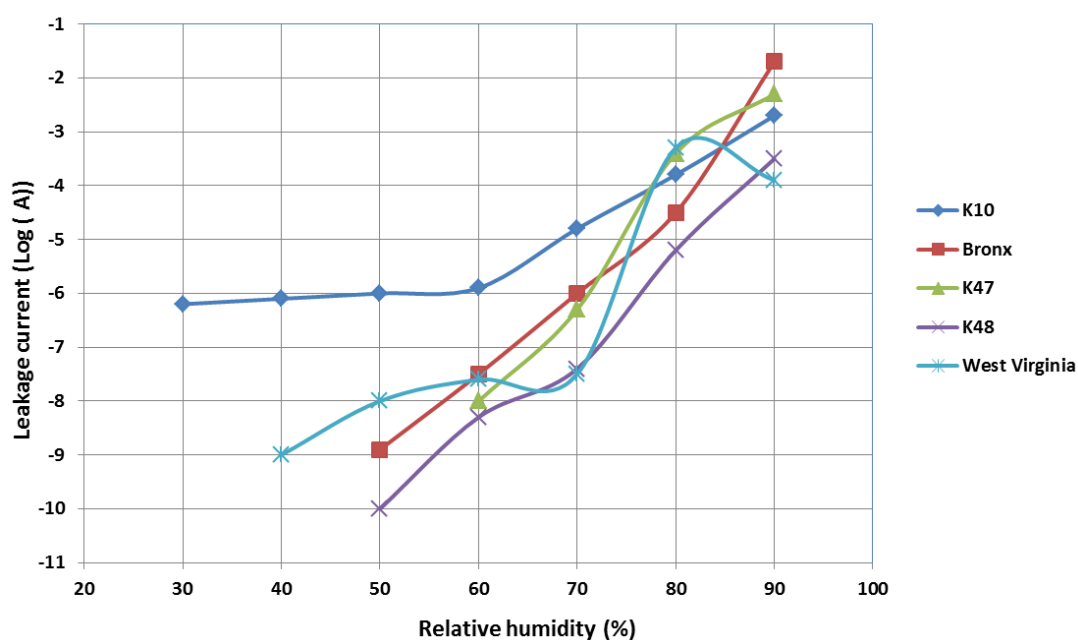


Figure 9. Effect of dust with soot and various conductive elements to the logarithm to a leakage current as a function of relative humidity. All of these samples were collected outdoors. K10 was a dust sample collected from US embassy in Kuwait, K47 and K48 from New York (Murray Hill), Bronx (New York) and W.Va (West Virginia) (re-drawn after Comizzoli et al. 1992).

## 2.5 Corrosion environment standards

Corrosion is a well-studied natural phenomenon which causes large problems in industry. Since the beginning of industrial revolution, when the usage of structural metals increased dramatically, it has been important to determine the reasons behind corrosion and how to classify the different environments the materials are exposed to. Different corrosion prevention mechanisms are needed for sheltered indoor environments and polluted industrial or seashore surroundings (Aromaa 2005, P. 96). In this chapter, most used corrosion standards are introduced.

One of the most widely used corrosion standard is ISO 9223, published by the International Organization for Standardization (ISO), whose headquarters is in Geneva, Switzerland who and has 163 member countries. This standard is designed to be more of a general standard, which is applicable around the world. Therefore, it is often used together with more specified standards to determine corrositivity and corrosion rates of inspected environments (Aromaa 2005, P. 25). These more case sensitive standards are specified after different branches of industry or different operating environments. A good example of these is IEC 60721-3-3 which is released and updated by International Electrotechnical Commission (IEC), a sister organization for ISO and its focusing on standards dealing with Electrotechnical industry. In United States alongside with ISO 9223 also standard ANSI/ISA-S71.04 is used. The main difference between ISO 9223 and two other standards is that the corrosivity is determined according to metal corrosion rate, while IEC 60721-3-3 and ANSI/ISA-S71.04 determine corrosion classes by border values for pollutants.

Hienonen and Lahtinen (2007, P. 74) propose following procedure, presented in figure 10, for corrosion analysis. In this procedure the environmental conditions are first determined with IEC 60721 standards, then the time of wetness (use time, when relative humidity is  $> 80\%$ ) and environmental impurity classification are determined by ISO 9223, and together with all this data the corrosivity in that conditions are determined.

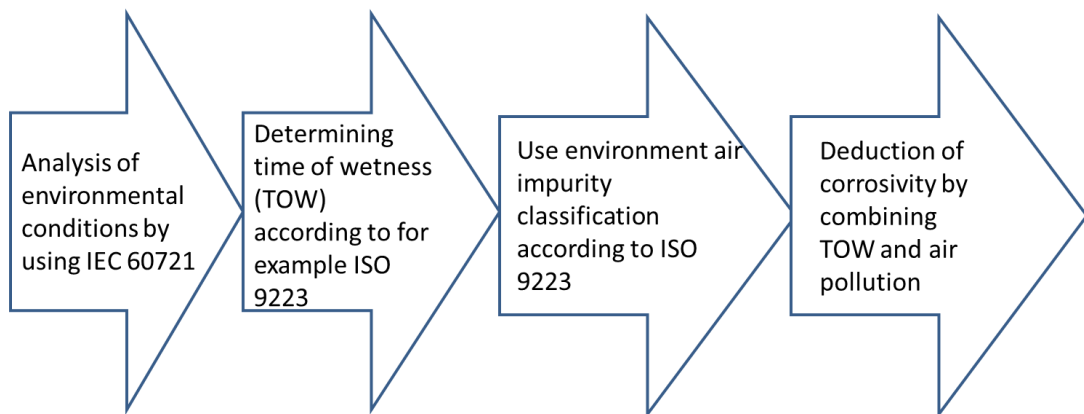


*Figure 10. A procedure for corrosivity determination (re-modelled after Hienonen and Lahtinen 2007, P. 74).*

### 2.5.1 ISO 9223

ISO 9223 standard classifies the corrosivity of an atmosphere based on measurements of time of wetness and pollution categories (sulfur dioxide and airborne chlorides). This standard is not intended to be used as a sole source for corrosion estimation for extreme service atmospheres, such as those within chemical or metallurgical processing facilities or where there is a direct contact with salt spray. However, it is a frequently used base standard for defining corrosion rates and the corrosivity of each environment to give a rough estimation of corrosion rates of metals. According to time of wetness (TOW) corrosion environments can be categorized in five (ISO 9223) or six classes (Henriksen et al. 1991) from mildest conditions ( $\tau_1$  like clean room environment to harshest conditions  $\tau_6$  tropical or greenhouse environment). TOW is defined in ISO classification as the percentage of annual conditions, where relative air humidity is  $> 80\%$  and temperature  $> 0^\circ\text{C}$ . (ISO 9223 2012).

*Table 4. Time of wetting classes according to ISO 9223 and Henriksen et al. (1991) own class distribution (Henriksen et al. 1991, P. 27.).*

Class according to ISO 9223	Class according to Henriksen et al. (1991)	Portion of the use time (%)	Example of occurrence
$\tau_1 \leq 10$	$\tau_1 \leq 10$	$\tau_1 < 0.1$	Internal microclimates without climatic control
$10 \leq \tau_2 \leq 250$	$10 \leq \tau_2 \leq 250$	$0.1 \leq \tau_2 \leq 3$	Internal microclimates without climatic control (except for internal non-air conditioned spaces in damp climates)
$250 \leq \tau_3 \leq 2500$	$250 \leq \tau_3 \leq 1000$	$3 \leq \tau_3 \leq 10$	Outdoor atmospheres in dry, cold climates or well ventilated indoor conditions
$2500 \leq \tau_4 \leq 5500$	$1000 \leq \tau_4 \leq 2500$	$10 \leq \tau_4 \leq 30$	Outdoor atmospheres in all climates (except for dry and cold climates)
$5500 \leq \tau_5$	$2500 \leq \tau_5 \leq 5500$	$30 \leq \tau_5 \leq 60$	Some zones of damp climates, unventilated sheds in humid conditions
-	$\tau_6 > 5500$	$\tau_6 > 60$	Green house

Based on these TOW classes and annual copper corrosion rates, six ISO 9223 corrosivity classes are defined. They are given in table 5. Corrosion rate means the oxidation rate of copper, which is assumed occurring by general corrosion, because it is easiest to measure, as the corrosion rate is almost uniform in it. In corrosion class C4 the corrosion rate is  $1.3\text{--}2.8 \mu\text{m/a}$ , which also the target range for corrosion tests done for this Master's Thesis. This rate is not enough to break copper traces whose thickness is minimally  $30 \mu\text{m}$ . However, this corrosion rate is defined from common corrosion and cannot estimate local corrosion mechanisms which electronics are more prone to. Common corrosion can promote formation of corrosion products which can cause short circuits or offer optimal conditions for local corrosion.

*Table 5. ISO 9223 corrosivity classes (ISO 9223 2012).*

Class	Corrosivity class	Corrosion rate in copper marked (r) (g/m <sup>2</sup> *a)	Corrosion rate in copper (r) (µm/a)
C1	Very low	$r \leq 0,9$	$r \leq 0.1$
C2	Low	$0.9 \leq r \leq 5$	$0.1 \leq r \leq 0.6$
C3	Medium	$5 \leq r \leq 12$	$0.6 \leq r \leq 1.3$
C4	High	$12 \leq r \leq 25$	$1.3 \leq r \leq 2.8$
C5	Very high	$25 \leq r \leq 50$	$2.8 \leq r \leq 5.6$
CX	Extreme	$50 \leq r \leq 90$	$5.6 \leq r \leq 10$

### 2.5.2 IEC 60721

Many of ABB drive product specifications use IEC 60721-3-3 standard to determine the limits for chemicals in their operation environment, while the two other parts of the same standard determine same limits while during transporting and warehousing, and these three forms the together IEC 60721-3. IEC 60721-1 lists environmental parameters (such as temperature, humidity, mechanical vibration) and IEC 60721-2 describes how these parameters alter around the world and gives their stress levels covering transport, storage and user conditions. (Hienonen and Lahtinen 2007, P. 74)

This standard classifies groups of environmental parameters and their severities to which products are subjected when mounted for stationary use at weather protected locations (IEC 60721-3-3 1994). ABB products are usually designed to meet the demands for Class 3C2 values, which are used as border values of chemically active substances for the operating environment for these drives. As can be seen from table 16, the list of these chemicals is almost identical between different corrosion standards and all of them mention already pre-mentioned Cl<sub>2</sub>, SH<sub>2</sub>, SO<sub>2</sub>, NO<sub>2</sub> gases. The sources for these pollutants can be industrial combustion processes and traffic but also natural volcanic activity is a great source of specially sulphur based compounds. Marine and seashore areas are usually heavily polluted by chlorine ions as well as Middle East desert salt which used to part of Mediterranean seabed some millennia ago. (Hienonen and Lahtinen 2007, PP. 14–15, 47–51)

*Table 6. Border values for chemically active substances according to IEC 60721-3-3. (IEC 60721-3-3 1994)*

Environmental	Class (Values as ppb)					
	3C1R	3C1L	3C1	3C2	3C3	3C4
Sea salts	None	No	No	Salt mist	Salt mist	Salt mist
SO <sub>2</sub>	37	37	37	110	1850	4800
H <sub>2</sub> S	1	7.1	7.1	7.1	2100	9900
Cl <sub>2</sub>	0.34	3.4	3.4	34	100	200
HCl	0.66	6.6	6.6	66	660	660
HF	1.2	3.6	3.6	12	120	120
NH <sub>3</sub>	42	420	420	1400	14000	49000
O <sub>3</sub>	2	5	5	22.5	50	100
NO <sub>2</sub>	5	52	52	260	1560	5200



### 2.5.3 ANSI/ISA-S71.04

This standard specifies the types and the concentration of airborne contaminants to which a specified instrument may be exposed. It is limited to airborne contaminants and biological influences only, covering contamination influences that affect industrial process measurement and control systems. (Hienonen and Lahtinen 2007, P. 202) The corrosivity classes for ANSI/ISA-S71.04 with border values of gaseous pollutants are given in table 7.

*Table 7. Air pollution classes in ANSI/ISA-S71.04 (Henriksen et al. 1991, P. 34).*

Class	Copper corrosion rate (nm/year)	Silver corrosion rate (nm/year)	H <sub>2</sub> S (ppb)	SO <sub>2</sub> /SO <sub>3</sub> (ppb)	Cl <sub>2</sub> (ppb)	NO <sub>x</sub> (ppb)	HF (ppb)	NH <sub>3</sub> (ppb)	O <sub>3</sub> (ppb)
G1	< 30	< 30	<3	<10	<1	<50	<1	<500	<2
G2	< 100	< 100	<10	<100	<2	<125	<2	<10000	<25
G3	< 200	< 200	<50	<300	<10	<1250	<10	<25000	<10
GX	> 200	> 200	>50	>300	>10	>1250	>10	>25000	>100

### 2.5.4 Standard summary and target corrosivity class in laboratory tests

As can be seen in tables 6 and 7, border values vary greatly between different standards. To give better understanding, how different corrosion classes correspond with each other, table 8 gives comparable corrosion classes in ISO 9223, ANSI/ISA-S71.04 and IEC-60721-3.

*Table 8. Comparable corrosion classes in three widely used standards (Hienonen and Lahtinen 2007, P. 83).*

ISO 9223	ANSI/ISA-S71.04	IEC 60721-3
C1	-	-
C2	G1	-
C3	G2	3C1
C4	G3	3C2
C5	GX	3C3

The combination effect of both time of wetness and pollution concentration can be found in figure 11. P classes are given in table 9. As can be seen by comparing P border values to IEC 60721-3-3 values, it can be seen that

P4 and P5 are close to 3C2 values. Taking into consideration that drives are sometimes subjected to high amount of pollution together with high humidity it was determined that the inspected area of the corrosivity graph would be in between harsh (G3) and severe (GX) areas.

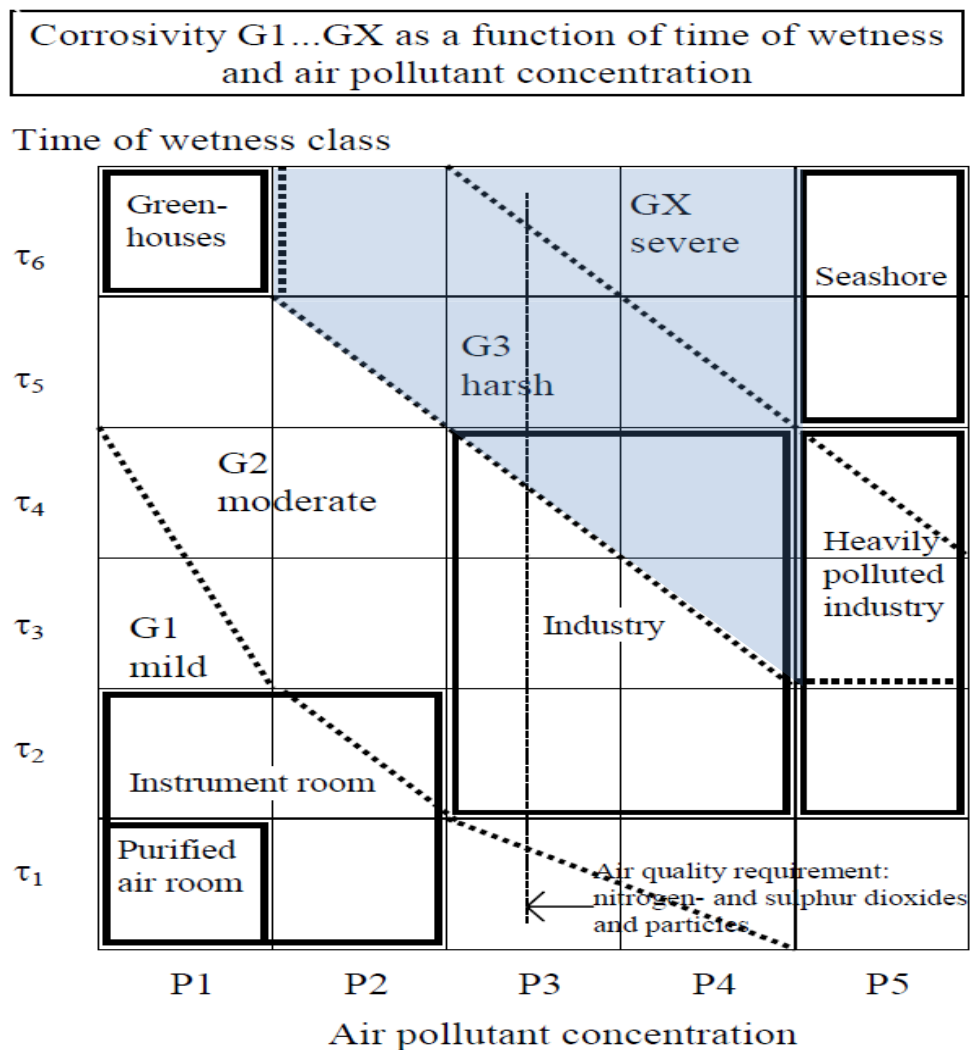


Figure 11. Corrosivities as function of time of wetness and air pollutant concentration. In the left side graph the limit values for ABB products (according to class 3C2 class in standard 60721-3-3) are marked with light red (Henriksen et al. 1991, P. 37)

*Table 9. Air pollution P classes in according to Henriksen et al. (1991, P. 31).*

Air pollutant classes	P1 (ppb)	P2 (ppb)	P3 (ppb)	P4 (ppb)	P5 (ppb)
Meaning	Very low	Low	Medium	High	Very high
SO <sub>2</sub>	3.8	10	38	114	> 114
NO <sub>2</sub>	13.25	80	265	530	> 530
H <sub>2</sub> S	3	15	71	142	> 142
Cl <sub>2</sub>	0.4	0.7	1.7	3.4	> 3.4
Cl-	0.4	1.7	3.4	17	> 17
NH <sub>3</sub>	14.3	358	1430	14300	> 14300
Soot	2	20	75	150	> 150

As examples of typical Nordic operation environments from different branches of industry with temperatures, relative humidities, corrosive pollutants and corrosivity classes according to ISA standard is given in table 10.

*Table 10. Corrosion conditions in different industrial locations. (re-made after Henriksen et al. 1991, P. 80–81)*

Outside (pbb)		Equip-ment rooms (pbb)	Fish indus-try (pbb)	Ani-mal shelter (pbb)	Or-dinary industry (pbb)	Severe indus-try (pbb)	Seaside (pbb)	Car indus-try (pbb)	Green-houses (pbb)
T (°C)	5	23	17	20	26	25	6.5	8	25
RH (%)	78	40	57	82	36	49	73	43	95
SO <sub>2</sub>	79	9	1	1	50	1447	11	5	0
NO <sub>2</sub>	53	32	81	45	111	43	28	57	8
H <sub>2</sub> S	6	7	10	56	44	188	1	1	1
Cl <sub>2</sub>	3	1	6	2	11	44	5	1	2
Cl-	1	2	36	21	7	39	1125	2	2
NH <sub>3</sub>	0	1	33	297	6	15	0	8	0
TO W P	τ5 - τ6 P2/1	τ1 - τ2 P1	τ2 - τ4 P2	τ5 - τ6 P3	τ2- τ3 P3/4	τ2 - τ4 P5	τ5 - τ6 P5	τ3 P2/1	τ6 P1
ISA	G3	G1	G2	GX	G3	GX	GX	G1	G2

## 2.6 Standardized corrosion tests

Corrosion can be inspected by field and laboratory tests. Field test is a practical and low-cost way for corrosion monitoring, but its downside is long test-time. Because of this, accelerated corrosion tests have been developed. These tests are fast as they last usually from few days to few weeks. Their other benefit is the chance to adjust environmental parameters (such as relative humidity, temperature and corrosion agents) and find out how they affect to corrosion in different materials. Their downside is high cost and other resources such as laboratory and trained personnel. Several accelerated corrosion tests are used in industry, which include from example ISO and IEC standards as well as different tests, which have the names of companies, who invented them. VTT corrosion hand book (Hienonen and Lahtinen 2007, P. 180) gives some of the most common used corrosion tests in table 11. Together with corrosive gases also moderate temperatures (usually between 25–40 °C) are used with high relative humidities (70–85 %). Weight increase column refers to copper coupons, whose weight change is used to determine, how well a monitored test set-up follows standard's guidelines. Copper coupons are described more in detail in chapter 4.1.

As can be seen, the gas concentrations is usually fairly small. If fast test time (1-14 days) is needed, also corrosion tests with high humidity and temperature can be used. Two examples of these tests consist of relative humidity of 85 % and temperature of 85 °C (85 °C/85 % RH) or relative humidity of 90 % and temperature of 40 °C. Usually no corrosive agents are used, because these tests are able to destroy electronics fast. Test samples must be protected by plastic encapsulation, or they destroy in a manner, which does not represent real-life situations (Hienonen and Lahtinen 2007, P. 109-110). The other harsher tests option is ISO 21207, which is meant to simulate marine environments and which combines bi-component mixed gas tests and salt spray tests (ISO 9227), while the time of one test cycle is one week.

Based on table 11, two most corrosive tests based on amount of corrosive gases used in these tests would be GR-63-Core Outdoor and Battelle III. The first mentioned test was developed by Telcordia Technologies and the latter by Battelle Labs. Telcordia has developed two corrosion tests to simulate corrosion for weather protected locations (GR-63-Core Indoor) and outside conditions (GR-63-Core Outdoor). Likewise, Battelle has developed different corrosion tests for different environmental conditions. Battelle II simulates conditions of light industrial environment, such as business offices while Battelle III represents moderate industrial environment, such as storage areas with poor environment control. (Zhao 2005, P. 18–19). As can be seen, both of these tests are quite similar, except that Battelle III uses higher humidity, and it does not contain SO<sub>2</sub>.

*Table 11. Commonly used mixed gas tests and their conditions: temperatures, relative humidities and gas concentrations in ppb (re-made after Hienonen and Lahtinen 2007, P. 180).*

Test name	T (°C)	RH (%)	SO <sub>2</sub>	NO <sub>2</sub>	H <sub>2</sub> S	Cl <sub>2</sub>	Weight increase (mg/(dm <sup>2</sup> day))
IEC 60068-2-60 (Method 1)	25	75	500	-	100	-	1.0 -2.0
IEC 60068-2-60 (Method 2)	30	70	-	200	10	10	0.3 -1.0
IEC 60068-2-60 (Method 3)	30	75	-	200	100	20	1.2 -2.2
IEC 60068-2-60 (Method 4)	25	75	200	200	10	10	1.2 - 2.4
GR-63-Core In-door	30	70	100	200	10	10	1.0 - 1.4
GR-63-Core Out-door	30	70	200	200	100	20	3.1 - 4.1
Battelle II	30	70	-	200	10	10	-
Battelle III	30	75	-	200	100	20	-

Together with standard tests given in table 11, ISO organization has presented a set of flowing gas tests in standard ISO 10062. This standard gives six methods (A–F) with different combinations of sulphur dioxide, hydrogen sulphide, nitrogen dioxide and chlorine. All the methods and their gas combinations are given in table 12. Two test variations are also provided for all methods

- 25 °C and 75 % RH or
- 40 °C and 80 % RH

*Table 12. ISO 10062 test methods and their gas combinations (ISO 10062 2007).*

Test methods	SO <sub>2</sub> (ppb)	H <sub>2</sub> S (ppb)	NO <sub>2</sub> (ppb)	Cl <sub>2</sub> (ppb)
A	500	-	-	-
B	-	100	-	-
C	-	-	-	20
D	500	100	-	-
E	200	-	500	-
F	500	100	-	20

In ABB drive manuals the acceptability limits for relative humidity in the presence of air pollutants are 5–95 % and no condensation allowed. The operating temperatures are usually from -15 to 55 °C (ABB 2013, a and b).

### 3 Insulation and conductor resistance

Corrosion can be monitored in several ways, such as by visual, mass change or electrical tracking, which is mostly done by measuring isolation, surface or conductor resistance. In this project resistance tracking was chosen, because it allows automatical measuring and data storage and it can be used both in laboratory and in the field without disturbing corrosion phenomena itself.

#### 3.1 Insulation resistance

Insulation resistance between two different copper traces can be used to evaluate the corrosion rates in PCB. However, it is important to remember that the conductive patterns always have a great variety of traces width and spacing. This variety needs to be taken into account when conductive patterns and insulation resistances of a printed board are designed and tested. In order to increase insulation resistance the length of a trace has to be decreased or the distance between the traces has to be increased.

The insulation resistance  $R_I$  ( $\Omega$ ), measures how well two electric currents flowing in two different traces can be kept separate in order to avoid a short cut. These currents can go via base material, medium material between these traces or the surface of PCB (surface current). It can be calculated via equation 1 (Hienonen and Lahtinen 2007, L 1/44), where  $\rho_{\text{medium}}$  is the resistivity of PCB base material ( $\Omega\text{m}$ ),  $L$  is the distance between two traces (m),  $s$  is the length of one trace (m) and  $t$  is the thickness of one trace (m),

$$R_I = \rho_{\text{medium}} * \frac{L}{s*t}. \quad (1)$$

Figure 13 give a graphical prescription of the dimensions used in formula 1, 2 and 4.

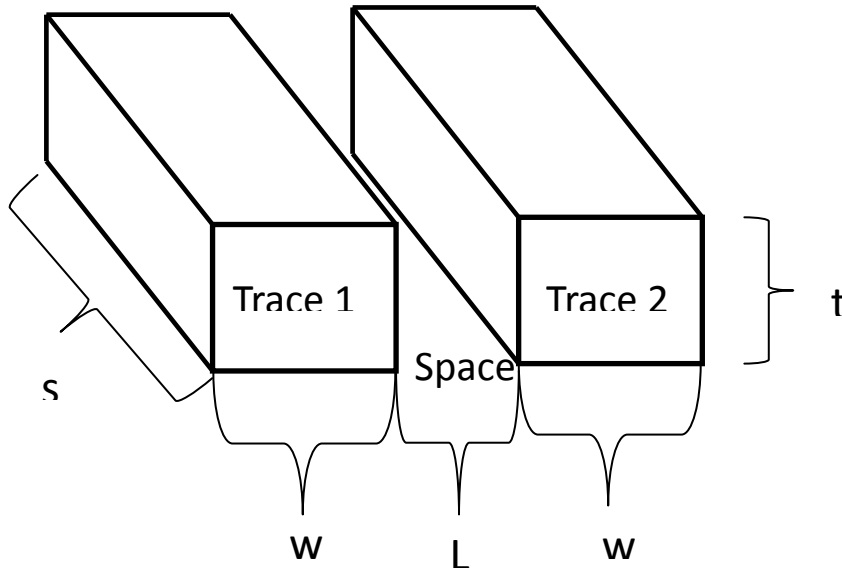


Figure 13. Dimension used in formulas 1, 2 and 4.

The insulation resistance of a printed wiring pattern is usually measured by using IPC testing patterns. For example the test board IPC-A-25 Multipurpose 1 & 2 Sided Test Pattern (IPC B-25) can be used for this purpose. (Hienonen and Lahtinen 2007, L 1/46)

### 3.2 Surface insulation resistance

Equation (2) (Hienonen and Lahtinen 2007, P. L1/46) gives a way to calculate the surface insulation resistance (SIR). In this formula  $\rho_{PCB}$  is the surface resistivity of the PCB ( $\Omega m$ ),  $s$  is trace length (m) and  $w$  is trace width (m), as presented in figure 13

$$R_P = \rho_{PCB} * \frac{s}{w} = \frac{1}{\sigma_{PCB}} * \frac{s}{w}. \quad (2)$$

SIR can be measured via comb like test structure described in IPC-9201 Surface Insulation Resistance Handbook and can also be calculated via equation (3) (Hienonen and Lahtinen 2007, P. 130), where,  $\pi$  is pi,  $f$  is the electrical frequency of the alternating current (Hz),  $\mu$  is magnetic permeability of the PCB base material (H/m) and  $\sigma$  is conductivity of the material (S/m),

$$R_P = \sqrt{\frac{\pi * f * \mu}{\sigma}}. \quad (3)$$

Surface resistance is therefore directly proportional to frequency and material properties of the surface but also contamination and conductive dust affect it greatly. Its recommended limit value for PCB is below  $2 * 10^8 \Omega m$  (Hienonen and Lahtinen 2007, P. L 1/52). PCB base material is usually made of a glass-reinforced epoxy laminate sheet, whose commercial name is “FR-4” This material’s conductivity is approximately 0.0042 S/m (Chen 2000) If length of a copper trace ( $s$ ) is for example 0.1 m and its width is  $100 \mu m = 1 * 10^{-4} m$ , then via formula 2

$$R_P = \frac{1}{0.0042 \frac{S}{m}} * \frac{0.1 m}{1 * 10^{-4} m} = 0.23809 ... * 10^6 \Omega = 0.23 * 10^6 \Omega. \quad (4)$$

### 3.3 Conductor resistance

The conductor resistance ( $R_C$ ) of one trace can defined with formula 5, where  $\rho_{Cu}$  is resistivity of copper,  $t$  is thickness (m),  $w$  is width of one trace (m) and  $s$  is the length of one trace (m)

$$R_C = \frac{\rho_{Cu} * s}{w * t}. \quad (5)$$

Conductor resistance can also be measured indirectly by measuring voltage between two ends of a trace when a known current ( $I$ ) flows through the trace. After that, conductor resistance can be calculated via Ohm's law, where  $U$  is the voltage over the trace (V),

$$R_C = \frac{U}{I}. \quad (6)$$

The resistivity of copper is directly proportional to temperature, and it can be calculated with formula 7, where  $\rho_{Cu0}$  is the copper resistance in a reference measurement temperature (usually 20 or 25 °C in literature),  $T$  is the use temperature (°C) and  $T_{room}$  is 20 °C.

$$\rho_{Cu} = \rho_{Cu0} * [1 + 0.004 * (T - T_{room})] \quad (7)$$

## 4 Corrosion Sensors

Various different kinds of sensors are available in the market today. A sensor is an appliance which reacts to stimuli (flow of heat, pressure or presence of chemicals etc.) and transforms the stimuli into an electronic quantity that can be measured. Corrosion is a complex process which rate can be estimated by monitoring factors causing or accelerating corrosion: the levels of relative or absolute humidity, temperature and corrosive gases and gas mixes. This is difficult because it must be determined how different gases affect to all drive materials and expensive due to high cost and amount of needed sensors and other equipment. The other way is to measure, how corrosion changes the function of the sensor, which can be electrical signal (resistance or conductance), mass change, or how mass change alters the natural frequency of the sensor. For simplicity laboratory tests can be first to solve how corrosion affect to the drive as a whole. Based on these results corrosion rates can be monitored in the field by direct corrosivity measurements (Prosek 2010).

Corrosion rate can be reported by annual mass change ( $\text{g}/(\text{m}^2 \cdot \text{year})$ ), thinning of copper thickness ( $\mu\text{m}/\text{year}$ ) or resistance change due to copper thinning and formation of insulative corrosion products. It is important to remember that the mass change can be resulted either by increasing or reducing weight, which is depended on whether the corrosion products stay or leave from the surface of corroding material. Corrosion rate measurements can be distributed into cumulative (mass change and coulometric measurements) and continuous types (quartz crystal microbalance and electrical resistance methods). Both these types are introduced next.

### 4.1 Mass change methods

Mass change methods (gain/loss), for example by utilizing copper coupons, are widely used in corrosion tests and standards to verify the corrosion rates and make sure that the test-set ups do meet the requirement (corrosion rates and allowed deviations from it) of the used testing standard. The problem with these mass change methods is that the mass change is a fairly crude method, which can underestimate the actual corrosion rate, if the corroding metal does not leave the surface and forms instead a compound between corrosive gases or other impurities.





*Figure 14. Copper corrosion coupons which can be used to monitor corrosion rates. These copper coupons were manufactured by Purafil and their dimensions are following: length is 10 cm, width 2 cm and thickness 5 mm.*

This mass change can be calculated via formula 8, where  $\Delta m$  is mass change (g) of a tested sample and  $A$  is surface area ( $m^2$ )

$$\text{weigh change in a sample as } \frac{g}{m^2} = \frac{\Delta m}{A}. \quad (8)$$

This mass change can be converted into an annual copper loss (m/a) by dividing it with copper's density ( $\rho_{Cu}$ )

$$\text{weight change in a sample as } \frac{m}{a} = \frac{\Delta m}{A} : \rho_{Cu} \quad (9)$$

In appendix A corrosion rates from two corrosivity tests are given. These tests were done in field in tropical conditions instead of in laboratory. The first test lasted for 16 years and the other had two separate, a year-long test period. The results copper corrosion rates were 1–4  $\mu m/a$ , which correspond with C4–C5 corrosion classes in ISO 9223 standard.

## 4.2 Coulometric methods

Coulometric measurements are done by electrochemical cell which includes electrolyte, wires, counter, reference and working electrodes and measurement devices (potentiometer and current meter). The working electrode the place where the measured chemical reaction occurs whose electrode potential is inspected by measuring the potential difference between the working and the reference electrode, whose potential is known. Because current cannot be allowed to pass the reference electrode, a counter electrode is needed. These measurements are used to measure corrosion potentials and currents (corrosion rates). Cumulative methods are usually simple and cheap to use but their downside is the long response time. Continuous methods are faster and more accurate but also more complex and expensive to use.

## 4.3 Quartz crystal microbalance

Quartz crystal microbalance is a novel and sufficiently sensitive method for indicating corrosion related changes and is used in the field (Prosek 2010). Principle of this method is given in figure 15. This method is based on measuring how corrosion changes the natural frequency of a metal coated crystal disc, when oscillator functions as a frequency source.

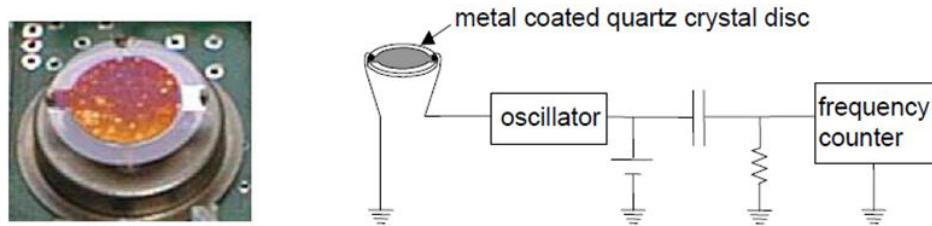


Figure 15. Principle of quartz crystal microbalance sensor, this sensor is based on measuring how corrosion changes the natural frequency of a metal coated crystal disc, when oscillator functions as a frequency source (Prosek 2010).

This method can be utilized by using equation 10, where  $\Delta f$  is the frequency change,  $f_0$  is the original natural frequency,  $N$  is frequency constant and  $\Delta m$  mass change (assuming film growth on one side of the crystal). The downside of this method is its sensitivity to temperature, humidity and dust, mechanical fragility and high cost.

$$\Delta f = - \left( \frac{f_0^2}{N * \rho_q} \right) * \Delta m \quad (10)$$

#### 4.4 Electrical resistance sensors

A structure of a sensor based on resistance change of copper trace due to corrosion is presented in figure 16. This method's advantage compared to quartz crystal microbalance sensor is its robustness and non-sensitivity to environmental disturbances (such as humidity, mechanical stress or temperature) and its downside is the slower response time. Electrical resistance sensor proposed by Prosek (2010) is based on measuring the resistance change between an uncoated and a coated electrical trace, which acts as a reference.

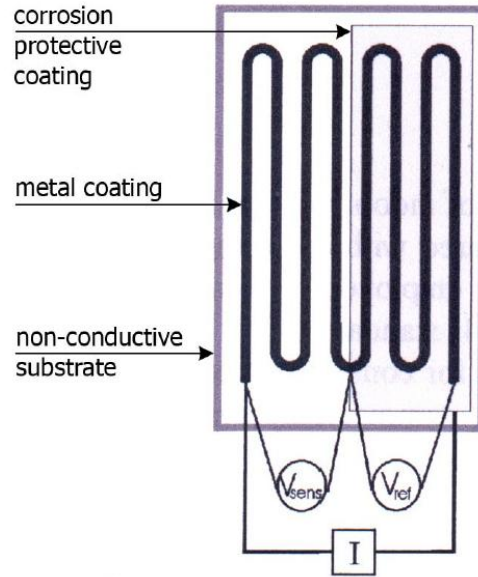


Figure 16. Electrical resistance sensor which consists of a corroding and a non-reacting reference area (Prosek 2010).

Corrosion depth can be calculated by formula 11 (Prosek 2010), where  $t_{init}$  is initial thickness,  $R_{ref}$  is the resistance of reference track,  $R_{sense, init}$  is initial resistance and  $R_{sense}$  is resistance of the sensor track

$$CD = t_{init} \left( 1 - \frac{R_{ref} * R_{sens, init}}{R_{sens} * R_{ref, ini}} \right). \quad (11)$$

In the case with PCBA, the initial trace thickness is hard to measure during manufacturing and it varies between different sensor units. Corrosimeters based on measuring the change of resistance are popular and several commercial applications and patents can be found. Because corrosion depth is hard to measure, instead of formula 11, resistance changes are usually directly measured and the measured value is compared with the stored initial value of resistance. In following chapter 4.41 different electrical are introduced.

#### 4.4.1 Electrical resistance sensor structures

Because the requirements mentioned in chapter 1.3 need to be met following conclusions could be made. To achieve a profitable price, a modified version of electrical resistance sensor had to be developed and tested in laboratory experiments. In this chapter electrical resistance sensor structures which were as a base for novel corrosiometer are presented. The novel corrosiometer is then presented in chapter 5.1.

The problem with mass change methods were their inaccuracy, while both coulometric and quartz crystal microbalance methods are too complex and expensive for the case of an environmental fuse. Electrical resistance corrosiometers were determined to be the most promising sensor type, but corrosion depth measurement was determined to be too variable to be properly predicted, so instead applications of direct electrical resistance measurements were decided to be examined. In this chapter the results of this survey are presented. As examples of standard IPC specimens, IPC 26-36-2, IPC-B-24 and IPC-B-25A multipurpose test board, are presented in figure 17.

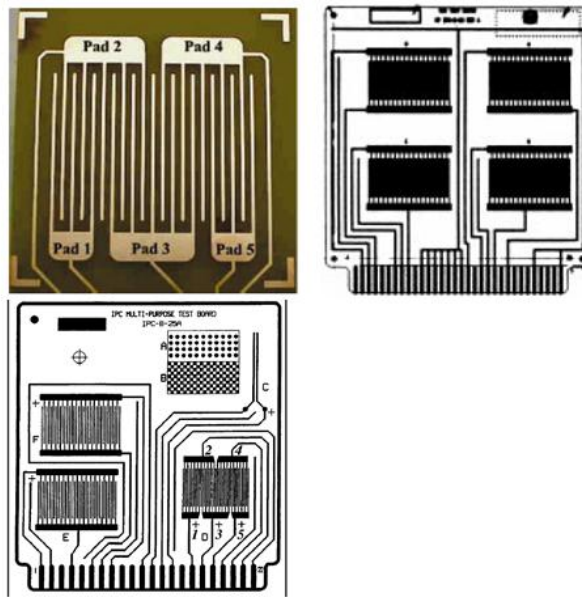


*Figure 17. IPC test boards used to measure insulation resistance. The green colored sensor is IPC 26-36-2, next to it is IPC-B-24 and below them is IPC-B-25A multipurpose test board (IPC-TM-650 Test Methods Manual 2013).*

The downside with these IPC patterns is that they measure only insulation resistance and do not tell how the corrosion affects the trace itself. The other problem with these test patterns is their suboptimal spacing, which is not dense enough for a corrosiometer which must fit in a small place available in PCBA.

The patterns for copper traces printed for PCB specimen were designed by utilizing standardized IPC patterns and Vahter pattern, which is presented in figure 18.

Vahter's pattern is made of three copper traces with varying width and spacing. The length of one trace is approximately 0.32 m. Three traces were used together to promote leakage currents between two traces, while the third trace could be used as reference.

The leak resistance can be calculated via formula 12 (Vahter 1999, P. 62), where  $R_{\text{leak}}$  is the leak resistance ( $\Omega$ ) and  $R_{\text{ref}}$  reference resistance ( $\Omega$ ) measure over neighbor copper trace,  $U_{\text{bias}}$  is input voltage (5V) and  $U_{\text{meas}}$  and is measured voltage, which is measured over two ends of a trace.

$$R_{leak} = \frac{U_{bias} * R_{ref}}{U_{meas}} - R_{ref}. \quad (12)$$

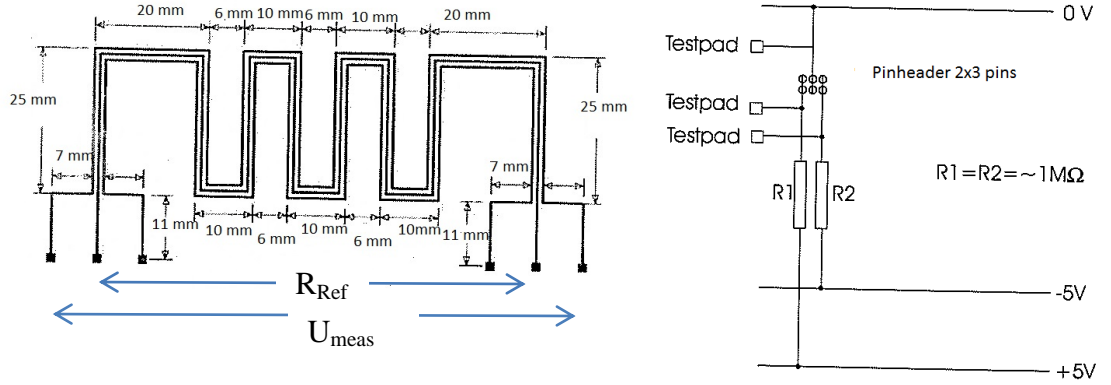


Figure 18. In left: copper trace pattern used by Vahter for conductor resistance calculations and measuring set-up used by Vahter (Vahter 1999, P. 63).

The test pattern proposed by Vahter is simple and easily manufacturable. However, the problems with this test pattern are the same as with the IPC test patterns as both measure only insulation resistance and take too much space from the PCBA.

Agarwala and Pearstein (1994) present a sensor structure which is thin enough to be situated between two layers of a laminated composite structure or beneath a coating. It is given in figure 18. According to inventors, this sensor is designed to be light enough to be suitable for aircraft environment. They propose that base material of this sensor can be made of polyimide sheets (Kapton, made by DuPont), which according to this patent description is available as thin as 0.025 mm, or glass-epoxy sheets with minimum thickness of 0.254 mm.

Agarwala and Pearstein (1994) explain that sensing patterns, which are drawn with black lines in figure 19, are made of two dissimilar materials, where the less noble acts as an anode and the noble as cathode. These patterns are made on an insulating surface, and when the surface is dry, there are no electrical paths between these patterns. However, in the presence of an electrolyte, consisted of condensated water and dissolved impurities, creates a galvanic potential between these two metals will generate galvanic current. The magnitude of this current will be indicative of the corrosivity of the electrolyte or environment.

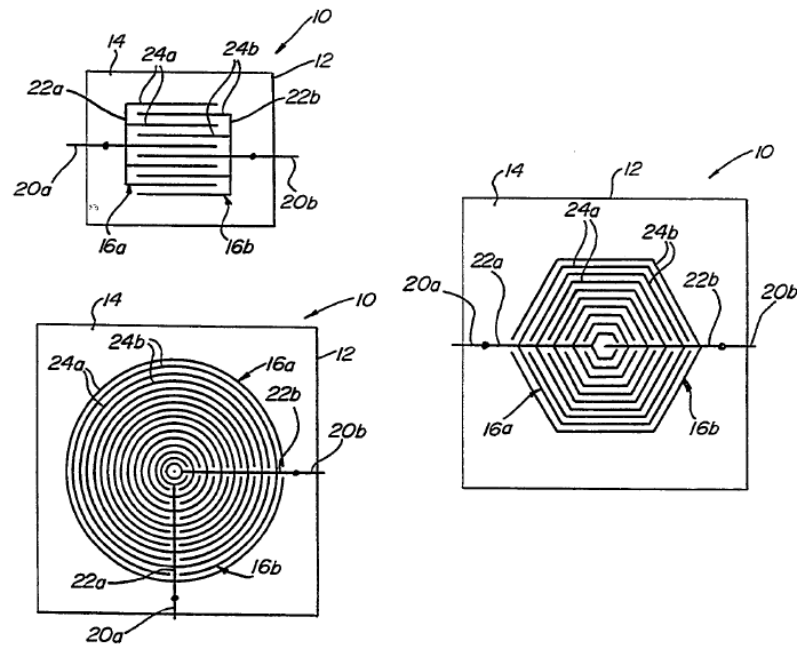


Figure 19. Corrosiometer for measuring insulation resistance proposed by Agarwala and Pearstein (1994).

The selection of the conductive sensing materials can be based on their relative electrochemical potentials or by what specific corrosive elements are being monitored. The metals may also be chosen to simulate the objects being corroded. One useful implementation employs gold and zinc as the cathode and anode, respectively, a combination which is very sensitive to the presence of small amounts of moisture. Even moisture generated from by breathing on such a gold–zinc sensor can be detected. This material combination was found to be most reproducible and responsive to humidity changes during long-term exposure because it produced a highly detectable current output (a few microamperes) even in below 80% relative humidity. Other useful metal combinations were found to be gold–iron, copper–zinc, gold–copper, tin–iron, nickel–chromium, and gold–cadmium. (Agarwala and Pearstein 1994).

The advantage of this sensor is its simple structure and operating principle. Its downsides are material pairs which include chromium, cadmium or gold which require special and expensive process steps to manufacture. In addition EU directive called “Restriction of the use of certain Hazardous Substances in Electrical and Electronic Equipment” (RoHS) has restricted the use of cadmium and hexavalent chromium ( $\text{Cr}^{6+}$ ) in electrical and electronic equipment from the June 2006, so these material choices are not practical. The other problem with the structure presented in this patent is the shortness of traces which makes conductor resistances too low to measure easily and at a reasonable price. It is also likely that this sensor gives a warning when corrosion has happened, but cannot predict or monitor how corrosion proceeds because electrical signal forms only when electrolyte is formed.

Jaeger 2003 presents a structure presented in figure 20. This corrosion sensor includes a support, a power source (marked as “110”), a visual indicator (marked as “120”), and an electrode (marked with “130”) having an electrical resistance contained on the support and coupled to the power source and the visual indicator. This sensor monitors the change in resistance and gives a visual signal of it. This display on the visual indicator can be either change of color or brightness. This method also includes monitoring changes in the display on the visual indicator. These changes in the display on the visual indicator are mark of corrosion of the monitored material. (Jaeger 2003)

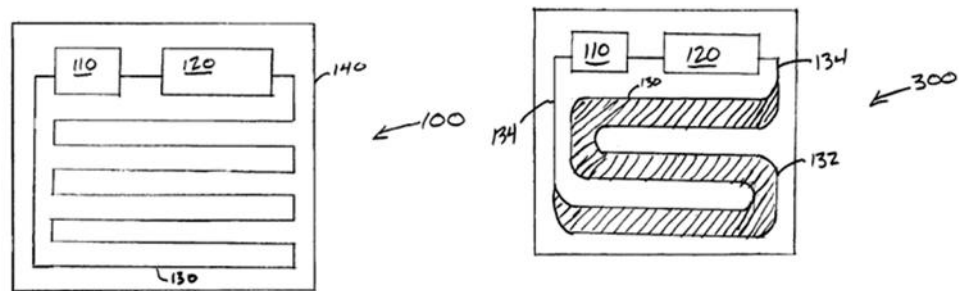
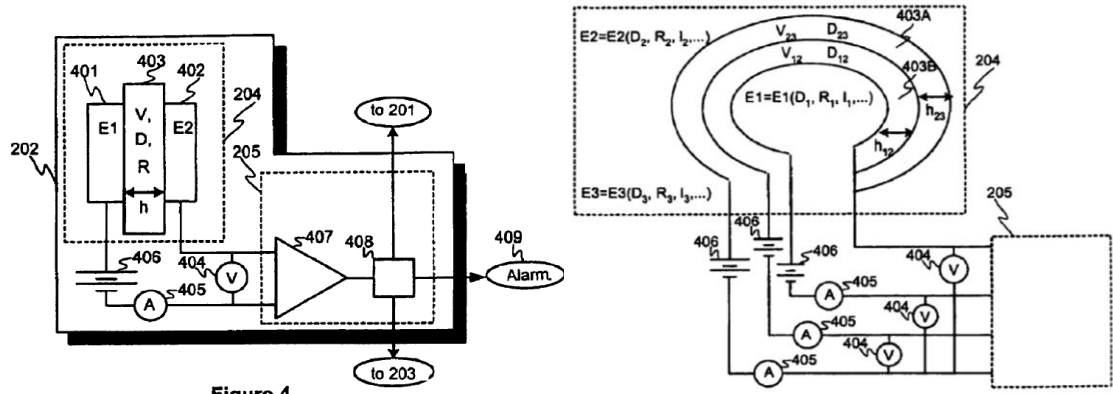


Figure 20. Corrosiometer presented by Jaeger 200. This corrosion sensor consists of a support, a power source (marked as “110”), a visual indicator (marked as “120”), and an electrode (marked with “130”) having an electrical resistance contained on the support and coupled to the power source and the visual indicator. (Jaeger 2003).

The material choices for Jaeger’s sensor vary. Electrode may be of any conductive material which is susceptible to corrosion. Electrode is usually made of a metal or metal alloy such as iron, aluminum, manganese, copper, carbon steel, silver, cobalt and molybdenum and alloys containing these metals. Any corrosion notified by electrode may be indicative of corrosion of surrounding materials. In one application electrode contains the same material as the monitored material in order to expose its corrosivity the used environment. For example, when a carbon steel support structure is monitored, electrode may contain carbon steel. (Jaeger 2003)

The advantage of the corrosiometer presented by Jaeger (2003) is that this corrosiometer measures directly the resistance change of the wanted material and this material can be chosen by using it as a corroding electrode. The downside in this option is the need for visual indicator, which is impracticable inside cramped spaced drives where visibility is limited and contactless corrosion monitoring systems would be more practical. The other problem with this sensor type is that it does not monitor the surface resistance on PCB.

ABB has patented a more complex corrosiometer called “environmental fuse” which is given in figure 21. This corrosiometer is based on an active layer marked as “403”, which changes its behavior (resistance, conductance or capacitance) according to presence of monitored gas, humidity or environmental phenomenon (corrosion or temperature etc.). If this change surpasses allowed tolerance, the active layer send a warning signal though connecting layers “401” and “402” and after this the signal is processed and saved into fuse’s memory and the environmental fuse gives a warning or restricts the operation of a motor actuator in order to prevent lasting damages to the motor.



**Figure 4**

Figure 21. ABB environmental fuse which is based on measuring changes of an active layer marked as “403”. Is this change is greater than allowed tolerance, this sensor given a warning restricts the operation of a motor (Silvennoinen 2010).

The benefit of this sensor system is its customizability and its ability to restrict the function of the motor if needed. Its disadvantages are its complexity and high cost. One problem can also be that if individual corrosive gases or humidity is used as a signal of corrosion, it is likely that corrosion mechanisms caused by other gases are missed in the process



## 5 Experimental

In this chapter corrosiometer designed and tested in this Master`s Thesis is presented followed by chosen tests standard and description of test set-up.

### 5.1 Proposed new corrosiometer structure

The requirements for the corrosion sensors (chapter 1.5) were following

- Operating temperature range  $-40 - +125^{\circ}\text{C}$
- Size of  $\leq 200\text{ mm}^2$
- Small price ( $\leq \$ 3$ )
- Sensor must be easily integrated in PCBA manufacturing process.

Because none of the options found from literature meet the demands given previously, a new corrosiometer needs to be designed and tested. The structure of this corrosiometer was designed after patterns presented by Vahter (1999) and Awargala and Pearstein (1994). This sensor structure is presented in figure 22. The first pattern is the source for the inner loop drawn with narrower line and the latter was the base for the comb like structure drawn with bolder line.

The loop is made from one long trace, with the length of 0.475 m, and it is used for measuring changes in conductor resistance. The comb like structure is used to measure the insulation resistance of PCBs as leakage current travels from loop structure toward the comb. This insulation resistance consists of both surface and bulk resistance but as Ready and Turbini (2000) state that in a case of FR-4, over 99 % of the current leakage will occur across the surface of the laminate. However, term “insulation resistance” has been used in result section because the comb structure cannot separate surface from bulk resistance.

Both of these patterns are made of copper. In figure 22 the loop structure seems to be wider than the comb, but this is due bended structure of the loop where the long trace is bended in the middle and so it forms the loop structure with two parallel traces. In reality loop`s trace width was 0.1 mm and the comb`s 0.2 mm, and the thickness of copper was 0.045 mm. Loop`s width and copper thickness are the smallest allowed dimensions in PCBs used by ABB to raise conductor and insulation resistance into an easily measurable level.

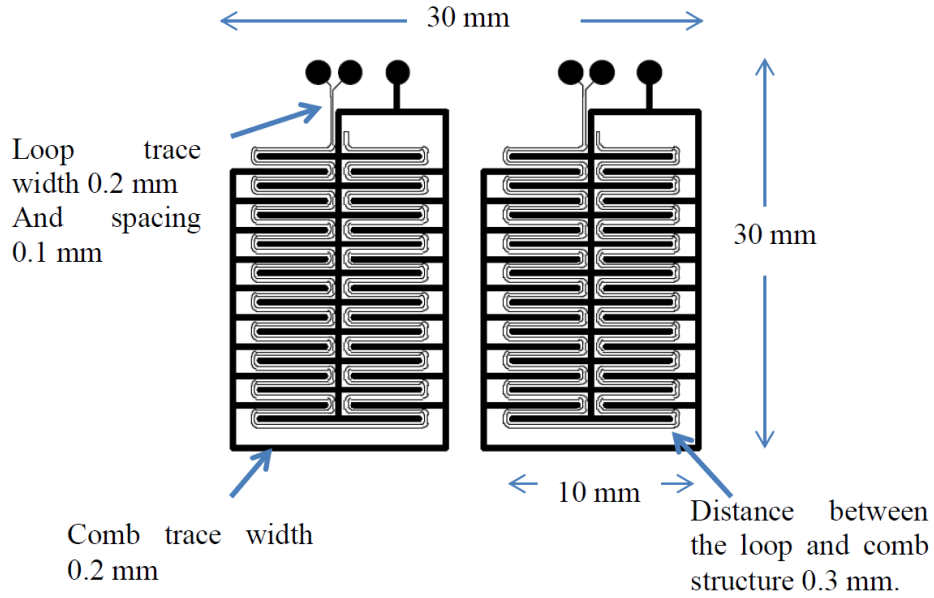


Figure 22. The corrosiometer designed for this Master's Thesis. This corrosiometer is made of two patterns: loop, which is made of a single long trace and the comb structure. The loop measures conductor resistance and comb insulation resistance

Together with the sensor structure additional patterns were inserted to the sample board to inspect, how corrosion affects to plated through hole (PTH), parallel and serial resistor and Quad flat package (QFP) structures, which all are common structures in PCBA. This whole test board structure is given in figure 23.

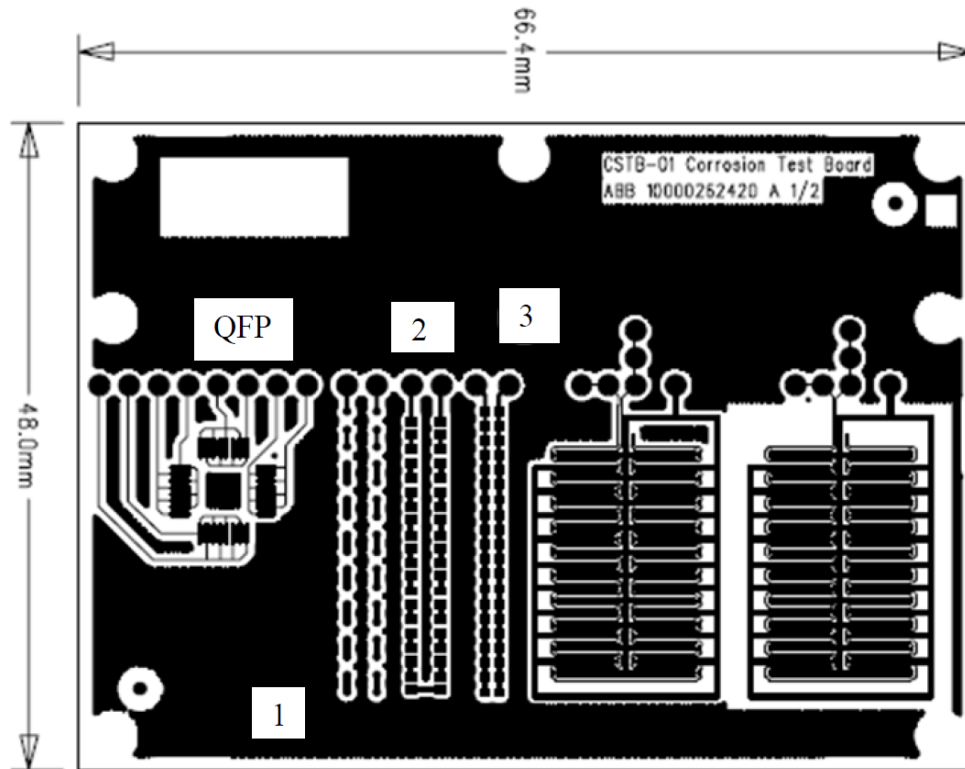


Figure 23. Testing patterns next to corrosiometer patterns (in right): QFP, PTHs (1), serial (2) as and parallel resistors (3).

PTHs are made of holes drilled through PCB plate. These holes are plated by a thin copper layer. They are used to connect electrically the two sides of PCB and their components. If this thin layer corrodes through, resistance of this pattern will increase, because then the current has to travel via the substrate material of PCB. In the field PTHs can be destroyed either by local corrosion or after humidity and temperature cycles have delaminated and swelled the PCB substrate which is made of polymer and glass fibre resin. The serial resistor patterns were made of connected small resistors (0–1  $\Omega$ ), and the parallel patterns made by connected large resistors (1–5 M $\Omega$ ). Densely connected QFPs were chosen to simulate how corrosion affects the connections between the PCB and its components. In practice PTHs and serial resistor test-patterns measure the conductive resistance of the pattern. Likewise, QFPs and parallel resistors pattern measure the surface resistance of these patterns.

## **5.2 Sample preparation and used material combinations**

Corrosion sensor samples manufactured via same processes as normal PCBs used by ABB. These samples were manufactured by Aspocomp Oyj. Four samples were prepared from each tested material combination: bare copper, immersion tin, solder resist and conformal coated copper traces. This means that 32 copper patterns were used for measuring conductor and insulation resistances. In addition 32 test patterns including PTHs, QFPs, serial and parallel resistors with uncoated and conformal coated cases were manufactured. In total 64 test patterns were used in this laboratory test. Sample numbers are given in appendix B.

Four different material combinations were used in testing. The idea was to use two corrosion cells together as a pair, in which the other would be made of corrosive material (bare copper or immersion tin plated copper), while the other would be coated with inert material (solder resist or conformal coating), which prevents corrosion. The idea was that the resistance signal from the corroding sensor would be compared with the reference signal to filter out any environmental disturbances, such as rapid temperature changes due to maintenance breaks. Immersion tin is used as a part of solder which attaches electrical components to PCB board. Solder resist is used before soldering to stop solder reaching place it is not wanted such as contactor areas. In standard manufacturing process conformal coating is added on top electrical assembly in order to stop humidity, corrosive gases or dust reaching vulnerable electronics below. It is commonly made from acrylate or epoxy.

## **5.3 Choosing test standard**

Because environmental tests are both expensive and time consuming, accelerated corrosion testing is used. However, the failure mechanism should be same as in the field. To achieve these, two options are available:

- To make testing conditions as harsh as possible (high temperature, high amounts of contaminations and/or humidity). Options : 85°C/85% RH tests, Salt spray tests or by
- Choosing a mixed flowing gas test which is a gentler than tests mentioned in option 1

Different test options are presented in table 13. Salt spray tests and 85°C/85% RH tests were determined to be too demanding for PCBs without plastic encapsulation. Corrosimeters without encapsulation would corrode too easily and in a different manner than in field, because these tests are used to simulate seashore or marine conditions, where electronics are always well protected. (Hienonen and Lahtinen 2007, P. 109). A mixed flowing gas test was decided to be used instead. At first ISO 10062 method F (with temperature 40 °C and RT 80 %) was proposed for a test set-up, but because the only available environmental chamber could only withstand relative humidity of 70 %, this standard was also discarded.

*Table 13. Environmental corrosion test set-ups and their benefits and drawbacks.*

Test	Benefits	Drawbacks
85°C/85% RH or Salt spray tests	Fast (testing time 1–2 weeks)	Severe test conditions, used mainly to simulate marine en- vironments for polymer hous- ing
ISO 10062 method F	Tropical condi- tions	Humidity level too high for available environmental cham- bers
GR-63-CORE	Widely used method	Is this test set-up harsh enough to cause corrosion fast enough?

The selected test standard was Telcordia GR-63-CORE outdoor standard, which is generally well known, widely used and recommended by the test laboratory in Aalto University. Aalto recommended GR-63-CORE outdoor test, because it used relative high temperature with the maximum allowed relative humidity in the environmental chamber (70 % RH). The other advantage of this standard is that the corrosion rate can be monitored via copper coupons. As stated in chapter 4.1 copper coupons are a crude way to measure corrosion rate, but as they are easy to use, they are widely used for corrosion monitoring both in field and in industry.

These test set-up specifications are presented in table 14. (GR-63-CORE 2002, Zhao 2005). Together with them are the limit temperature, relative humidity and gas concentration values given for the environmental chamber used for these laboratory experiments. Aalto recommended a version of GR-63-CORE Outdoor with higher gas concentrations, because the actual flow of gases into the chamber could not be measured.

*Table 14. Specifications for Telcordia GR-63-CORE and limit values for used environmental test chamber.*

Name	Temperature (°C)	RH (%)	Cl <sub>2</sub> (ppb)	H <sub>2</sub> S (ppb)	SO <sub>2</sub> (ppb)	NO <sub>2</sub> (ppb)
GR-63-CORE outdoor recom- mended by Aalto	30	70	55	330	350	350
GR-63-CORE outdoor	30	70	20	100	200	200
Test chamber (max)	85	70	85	330	850	400

Table 15 presents the gaseous limit values for GR-63-CORE Outdoor field environments are given. For comparison, most widely used environmental corrosivity classes and their contaminant values for IEC 60721-3-3 (3C1 and 3C2) and ANSI/ISA-S71.04 (G3) standards are also given. Limit values for ISO 9223 standard categories are not given, because they are determined by corrosion rate instead of contaminant levels. As can be seen, all classes are close to fairly close to each other.

Table 15. *Telcordia GR-63-Core use environment contaminant levels (Zhao 2005).*

Standard	GR-63-CORE	IEC 60721-3-3		ANSI/ISA-S71.04
Contaminants	Outdoor environment (ppb)	3C1 (ppb)	3C2 (ppb)	G3 (ppb)
SO <sub>4</sub>	79	-	-	-
NO <sub>2</sub>	23	52	260	125 - 1250
SO <sub>2</sub>	150	37	110	100 - 300
H <sub>2</sub> S	40	7.1	7.1	10 - 50
NH <sub>3</sub>	50	420	1400	10000 - 25000
NO, NO <sub>2</sub>	750	5	22.5	125 - 1250
HNO <sub>3</sub>	50	-	-	-
O <sub>3</sub>	250	5	22.5	10
Cl <sub>2</sub>	6	3.4	34	2 - 10

#### 5.4 GR-63-CORE correspondence with use life and achieved resistance changes

GR-63-CORE standard (2006, P. 4–29) states that 14 test days corresponds with 20 years in field in GR-63-CORE outdoor environment or in G3 or 3C2 environment. Therefore the 28 days test simulates approximately 35–40 years in field. Henriksen et al. (1991, P. 57) note, that Battelle III and identical IEC 60068-2-60 (Method 3) tests, whose corrosivity on test coupons is approximately a half of GR-63-CORE outdoor (See table 11, P. 27), correspond with 10 years in field with 20 test days, so 28 days test time would correspond with 15 years in field. If the double corrosivity of GR-63-CORE is taken into account, then 28 days test time simulate 30 years in field. However, because neither of them includes sulfur dioxide (SO<sub>2</sub>), these two standards cannot be directly compared with the aging factor of GR-63-CORE. To give estimation, how corrosion affects to the corrosion, if maximum weight sense of copper coupon is approximately  $4.1 \text{ mg}/(\text{dm}^2 \cdot \text{d}) = 0.41 \text{ g}/(\text{m}^2 \cdot \text{d})$ , then the weight change in typical 30 days test is,

$$\Delta g = 0.41 \frac{\text{g}}{\text{m}^2 \cdot \text{d}} * 30 \text{ d} = 12.3 \frac{\text{g}}{\text{m}^2}, \quad (13)$$

The density of copper ( $\rho_{\text{Cu}}$ ) is approximately  $8960 \text{ kg}/\text{m}^3 = 896 * 10^4 \text{ g}/\text{m}^3$ . By using formula 9, the copper corrosion rate is

$$\frac{\Delta g}{\rho_{\text{Cu}}} = \frac{12.3}{896 * 10^4} * \frac{\text{g}}{\text{m}^2} * \frac{\text{m}^3}{\text{g}} = 1.37277 \dots * 10^{-6} = 1.37 \mu\text{m}/\text{month}. \quad (14)$$

In table 16 theoretical resistance changes are calculated with given theoretical corrosion rate and  $0.1 \Omega$  resistance change is got. This resistance change is easy to measure with right equipment.

Table 16. Theoretical conductor resistance ( $\Delta R_C$ ) changes with a corrosion rate of 1.37  $\mu\text{m/month}$ .

Sample	Length (m)	Thickness ( $\mu\text{m}$ )	Width ( $\mu\text{m}$ )	Area (m)	$\rho_{\text{Cu}}$ in 20 and 30 °C ( $\Omega\cdot\text{m}$ )	R in 20 °C ( $\Omega$ )	R in 30 °C ( $\Omega$ )
Reference	0.48	45	100	$4.5\cdot 10^{-9}$	$1.7\cdot 10^{-8}$	1.7	1.8
Gas-tested	0.48	44	97	$4.3\cdot 10^{-9}$	$1.8\cdot 10^{-8}$	1.8	1.9
					$\Delta R_C$	0.1	0.1

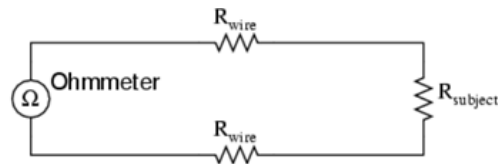
## 5.5 Test set-up and equipment

The test set-up consisted of following equipments:

- Environmental chamber and corrosive gases ( $\text{SO}_2$ ,  $\text{S}_2\text{H}$ ,  $\text{NO}_2$  and  $\text{Cl}_2$  )
- Developed corrosion sensor samples
- Electronical components such as Liquid Crystal Displays (LCDs), connectors with different platings and small PCBs were added into the chamber as reference samples to simulate how electronics behave in a corrosion test
- Monitoring equipment including two data loggers, wires and an separate humidity–temperature sensor to ensure right test conditions
- Copper coupons for corrosion rate measurements.

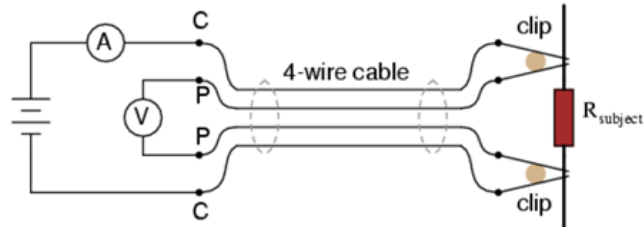
Measuring set-up consisted of two-point and four-point resistance measurements (Kelvin method) sensing methods, which are presented in figure 24. In two-point method, the ohmmeter is connected in series via with the test sample while in four-point method, separate voltmeter and ammeter is connected parallel with test sample, and resistance is calculated via Ohm's law.

Only insulation resistances were measured via four point method and all others using two-point method. Only direct current was used in these measurements. Measuring supplies were two pieces of Agilent 34970A Data Acquisition/Switch Unit loggers. The four-point measurements were carried out with Agilent 34901A 20 channel multiplexer cards (two pieces) and two-point measurements with Agilent 34908A 40 channel multiplexer measuring cards (two pieces). All the measuring channels had a shared ground.



Ohmmeter indicates  $R_{\text{wire}} + R_{\text{subject}} + R_{\text{wire}}$

#### Two-point measurement



$$R_{\text{subject}} = \frac{\text{Voltmeter indication}}{\text{Ammeter indication}}$$

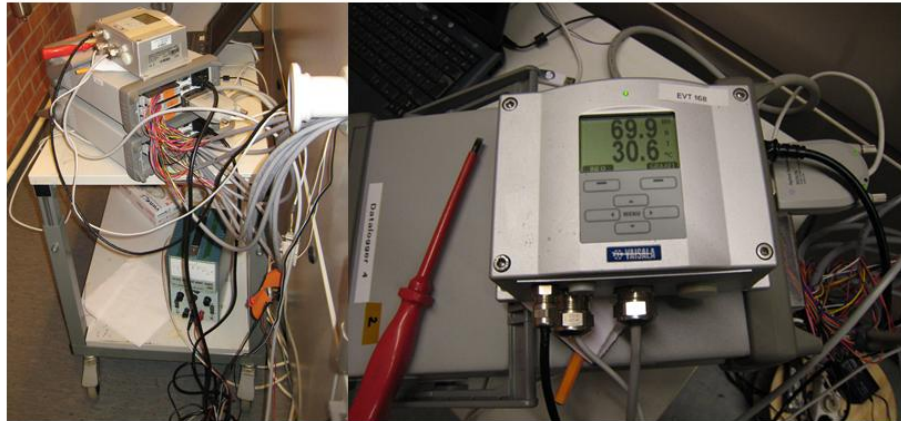
#### Four-point measurement

Figure 24. Two- and four-point measurement principle. In two-point method, the ohmmeter is connected in series via with the test sample while in four-point method, separate voltmeter and ammeter is connected parallel with test sample, and resistance is calculated via Ohm's law (Hæggström, Paulin, and Holmström 2013).

In figure 25, the environmental chamber WEISS WK 600 is presented. The white panel is the controlling unit and the data loggers are the grey boxes with wires in the left. On top of the data loggers is a separate humidity and temperature sensor. A closer view of the two data loggers and (left) and the humidity-temperature sensor is presented in figure 26.



*Figure 25. The environmental chamber from outside and white control panel.*



*Figure 26. Data loggers and the humidity–temperature sensor.*

A closer view of the control panel is presented in figure 27. As can be seen, this panel shows current date, time, chamber temperature and humidity. Because the chamber had been opened prior taking the figure 27, the control panel does not show its relative humidity.

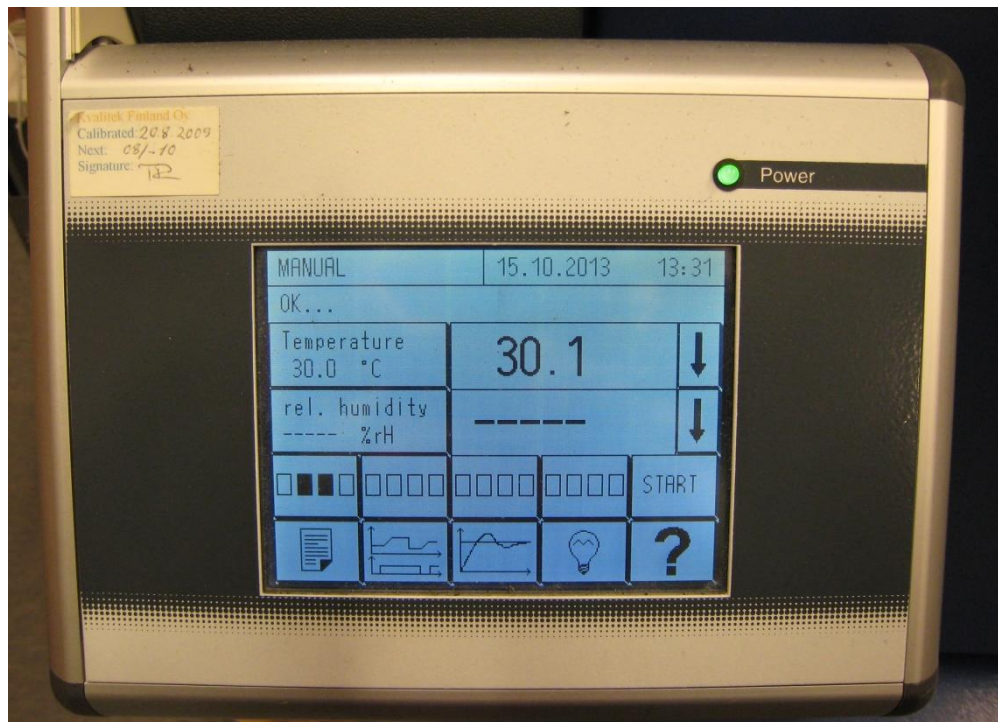


*Figure 27. Environmental chamber control panel with temperature and relative humidity adjustment.*

The environmental chamber consists of two nested chamber. Two chambers are used to stop the poisonous gasses from escaping outside or corroding the chamber itself. The inner chamber and specimen are given in figure 28.



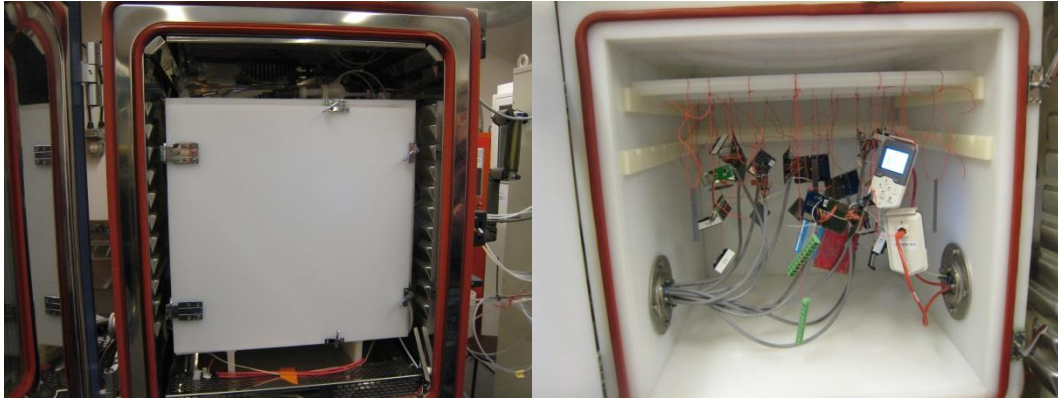


*Figure 28. Specimen and inner chamber before and after opening the door of the inner chamber. Two nested chamber structure was used in order to stop poisonous gases escaping from the chamber structure.*

## 6 Results

The results from the Telcordia Outdoor laboratory test are presented in this chapter. The Test was carried out in Aalto University in October-November 2013 and it lasted for 28 days. The test successfulness was followed by separate copper coupons and a separate humidity–temperature sensor, which stated that humidity and temperature values stayed in  $30 \pm 1$  °C temperature and  $80 \pm 1\%$  relative humidity. Due to problems with gas supply to the environmental chamber and large sample amount, the corrosion rates of the copper coupons were approximately half of the expected. However, according to Aalto environmental chamber expert Markus Turunen, the test results can be deciphered as if test time was 14 instead of 28 days. GR-63-CORE standard states that this test time corresponds to 15–20 years in field conditions described by the same standard. As usage conditions in GR-63-CORE and G3 are close to each other, it can be estimated that this test-set up corresponded with 15 –20 years in G3 conditions.

For better understanding of corrosion rates of copper traces, two cross section-samples were prepared from bare copper sensors. The first sample was done from untested sample and the other was from a sensor, which had been in chamber for four weeks. These samples were inspected with a scanning electron microscope (SEM).

### 6.1 Corrosion sensor resistance

In this chapter the sensor signal changes during the four weeks testing time are presented. Two samples for corroding sensor were bare copper and immersion tin coated copper. The non-reactive reference options were solder resisted and conformal coated copper traces. Copper conductor resistances with different material options are presented first and after them results from insulation resistance sensors are given.

#### 6.1.1 Conductor resistance

Bare copper conductors proved to react best in corrosion test while immersion tin coated copper showed very slight increase, but as change is less than 1 %, it is not significant enough for sensor structure. Both reference materials choices operated well in this test and did not corrode. This also means that the reference material coating can be chosen according to what is most practicable considering other manufacturing steps of PCBA. Bare copper conductor resistances are presented in figure 29. Conductor resistances for immersion tin coated traces are presented in figure 30, solder resist coated traces in figure 31 and conformal coated traces in figure 32.

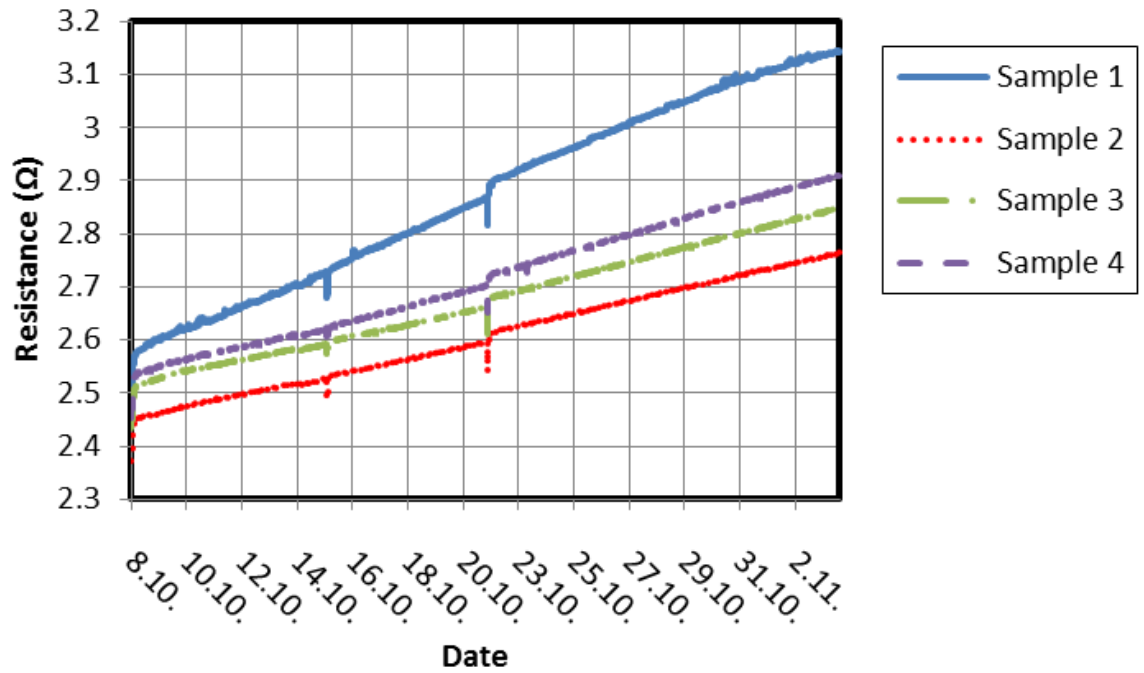


Figure 29. Conductor resistance of bare copper traces which change almost linearly. The small jolts are resulted from opening the chamber because of maintenance breaks.

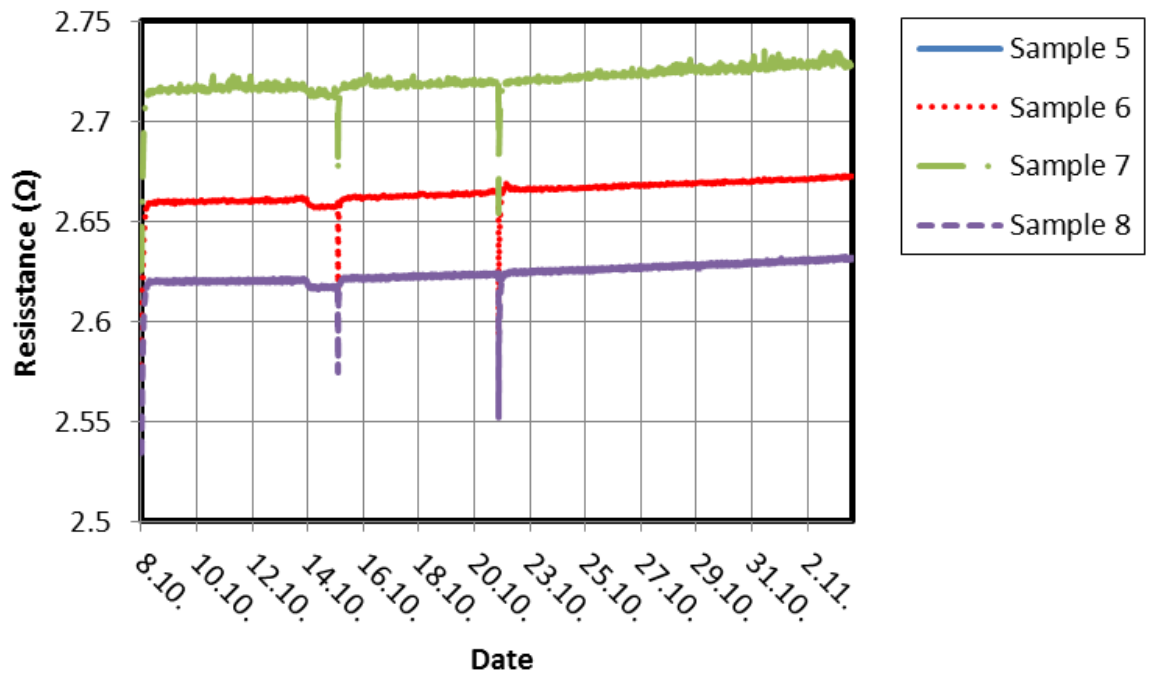


Figure 30. Conductor resistance of copper traces with immersion tin coating. The small change ( $< 1\%$ ) is not significant enough for the corroding part of the corrosiometer.

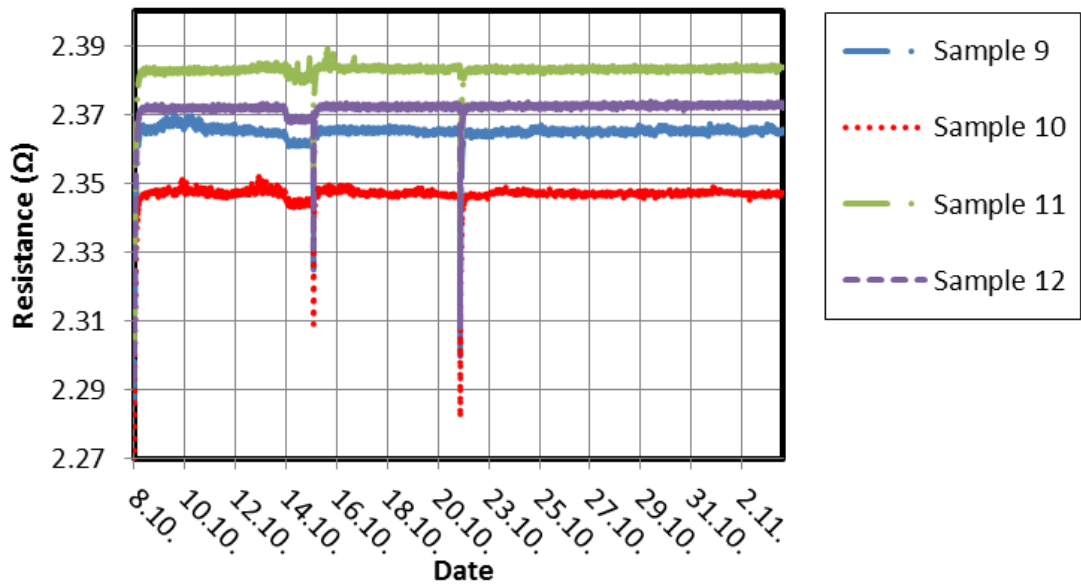


Figure 31. Copper traces with solder resist coating. These did not show change apart from jolts caused by maintenance breaks.

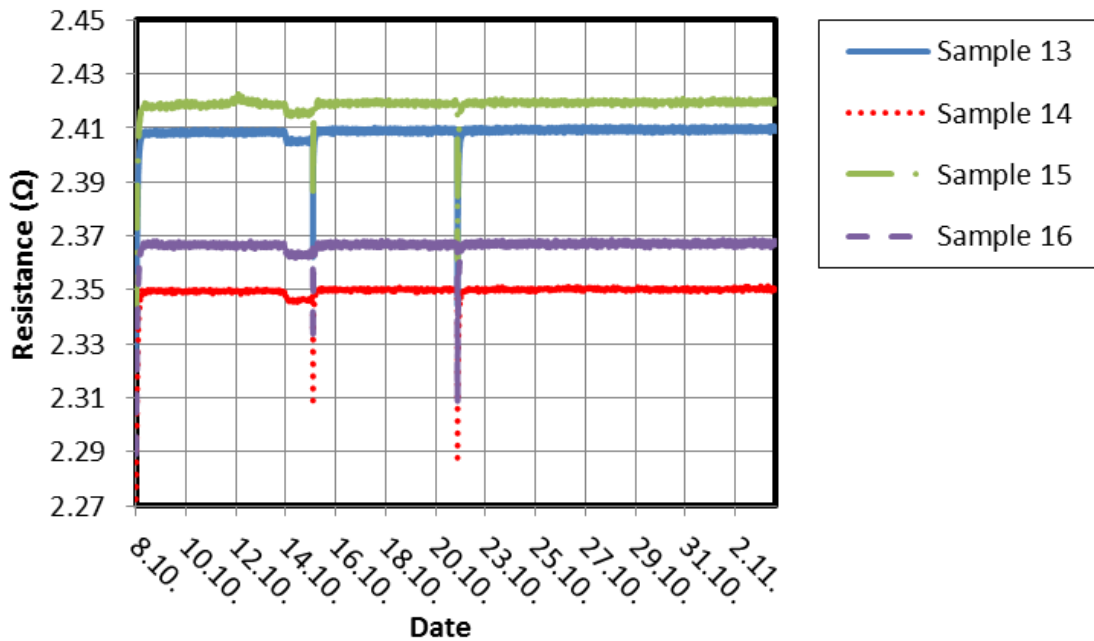


Figure 32. Copper traces with conformal coating. Their signals did not show change apart from jolts caused by maintenance breaks

All of the curves show peaks which are due to opening the environmental chamber during maintenance, which suddenly decreased temperature inside. By taking a subtraction between bare copper and reference signal all these peaks could be removed and almost linear signals could be obtained. In graph 33 this is demonstrated by choosing the most and the least changing bare copper trace signal and subtracting them with reference signals. The signals for the two other bare copper traces would stay in region between these upper and lower boundary lines. These bare copper traces would be good for life cycle estimations

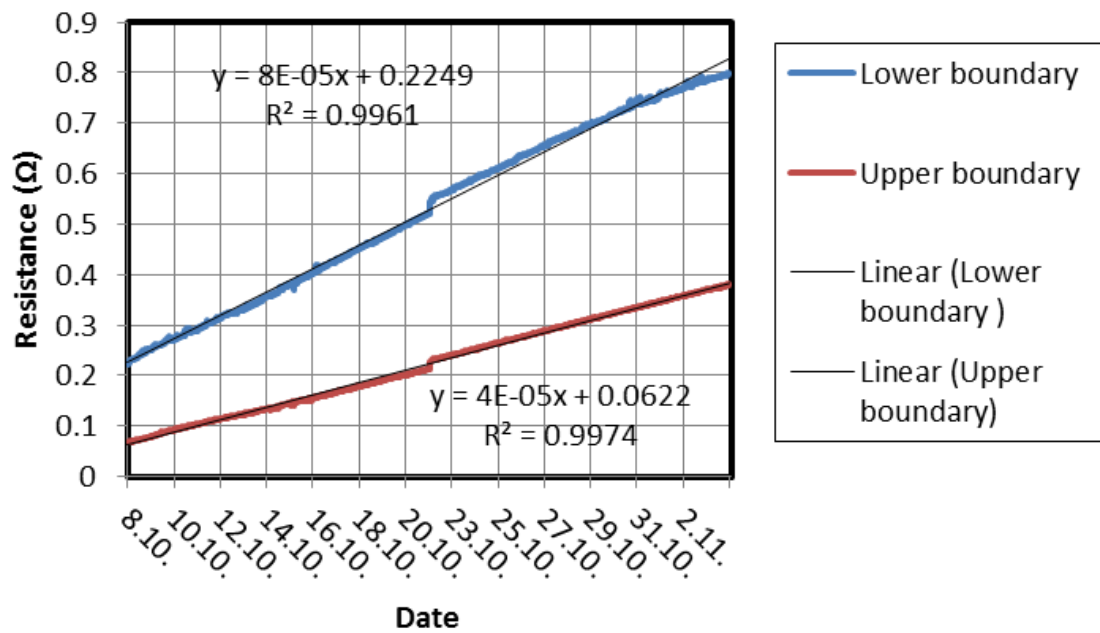


Figure 33. Bare copper trace signals after differential subtraction from reference signals. As can be seen in trend lines and their fit equations, maintenance jolts can be removed by differential subtraction.

### 6.1.2 Insulation resistances

Bare copper insulation measurements, given in figure 34, were only ones to give clear decline in surface resistances. Immersion tin coated traces showed decline, as can be seen in figure 35. However, as this signal stays over 10 MΩ, it was not clear enough for condition monitoring. Selected measuring range proved to be too low to measure changes in solder resist or conformal coated traces. As can be seen in figures 41 and 42, these changes are not linear. This occurs because surface resistance is very susceptible for environmental changes, such as surface contamination by corrosion products, corrosive agents or conducting dust. The problem with measuring insulation resistance was the correct choice of measuring range. Both of the reference material combinations did not show any measurable signal or change.

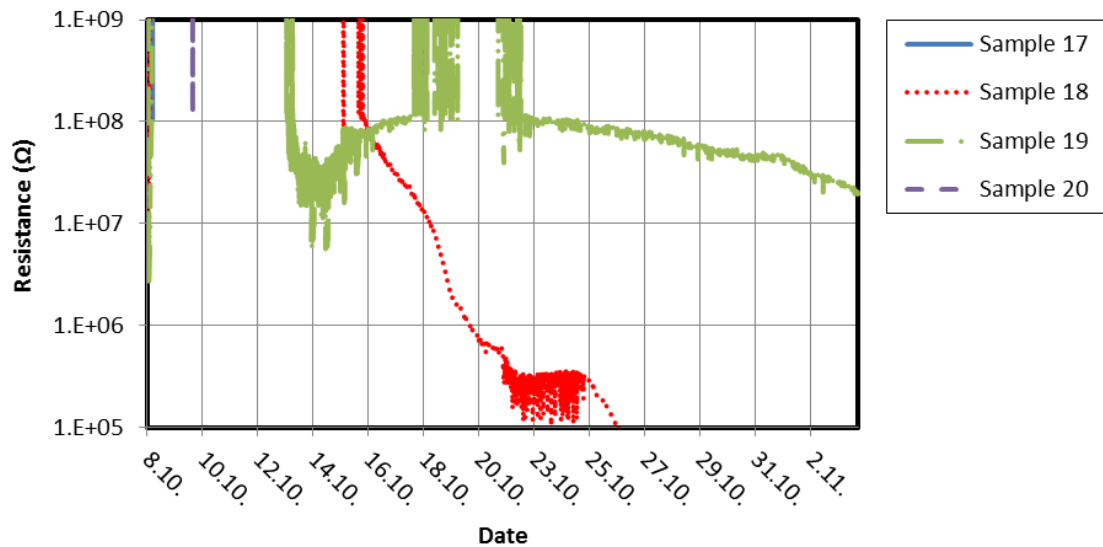


Figure 34. Bare copper insulator resistance during 28 days test time. Bare copper traces were the only material choice to give clear change during testing.

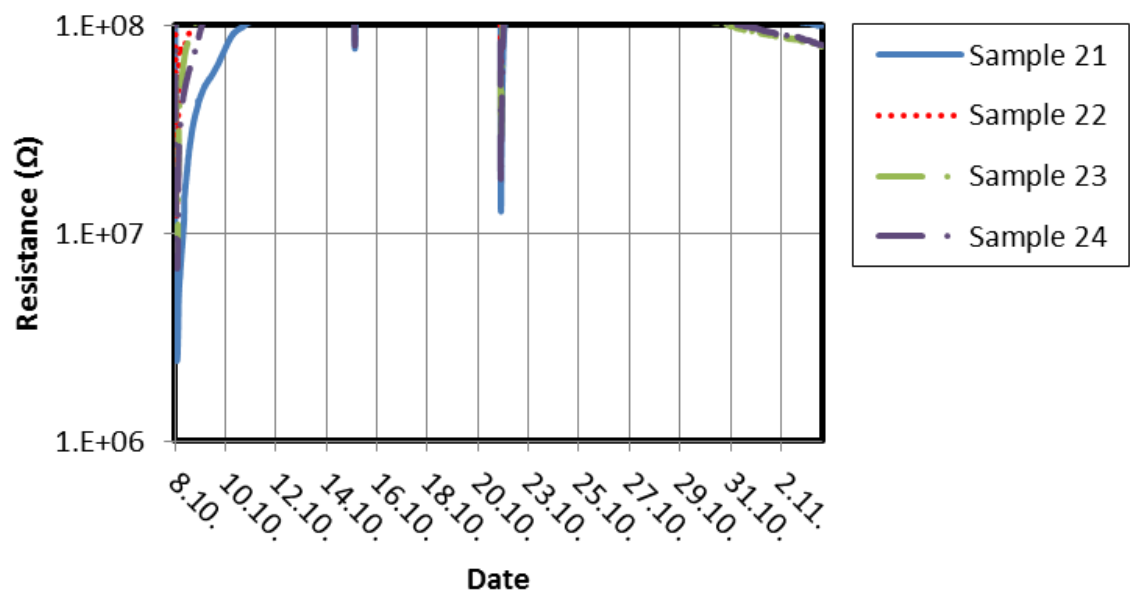


Figure 35. Insulation resistances of immersion tin coated copper traces. Small changes can be seen but the measuring range proved to be too low for proper condition monitoring.

## 6.2 Reference components

### 6.21 Plated through holes

The vias or plated through hole structures were chosen to inspect how corrosive gases are able to locally destroy the thin conductor layer on the surface of holes which are drilled through a PCB plate. The results for uncoated and conformal coated PTH patterns are given in figures 36 and 37.

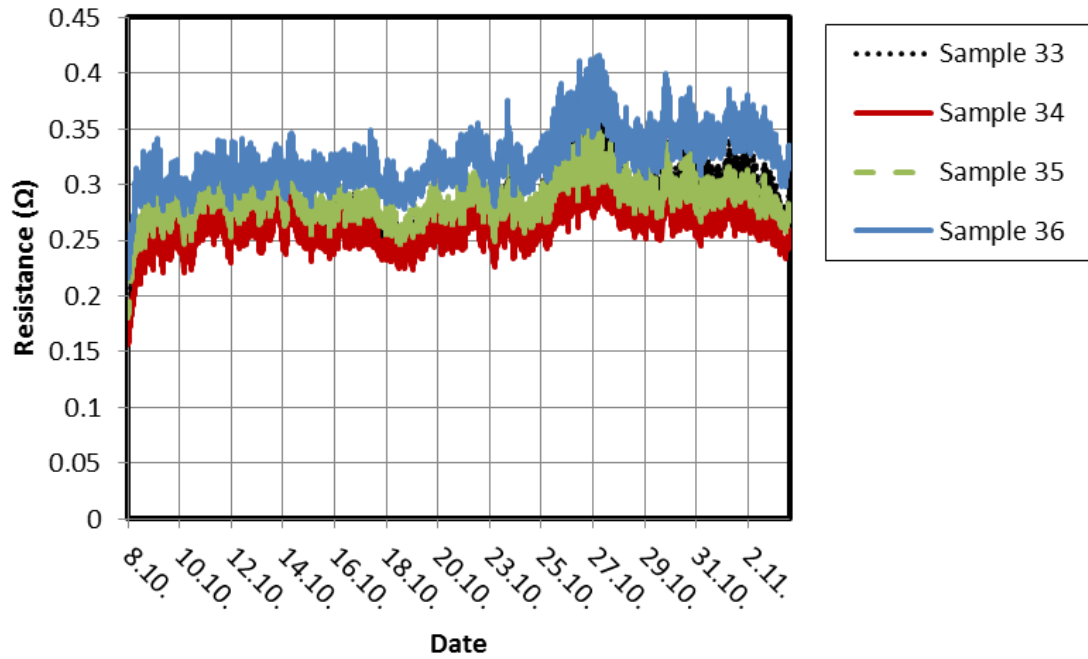


Figure 36. The resistance changes of plated through hole test patterns without conformal coating. There was no clear change during testing.

In these two cases it can be seen that the PTHs were not destroyed either in uncoated or conformal coated cases. The only effect that the conformal coating has is that the surface resistances are a little lower than with the uncoated cases.

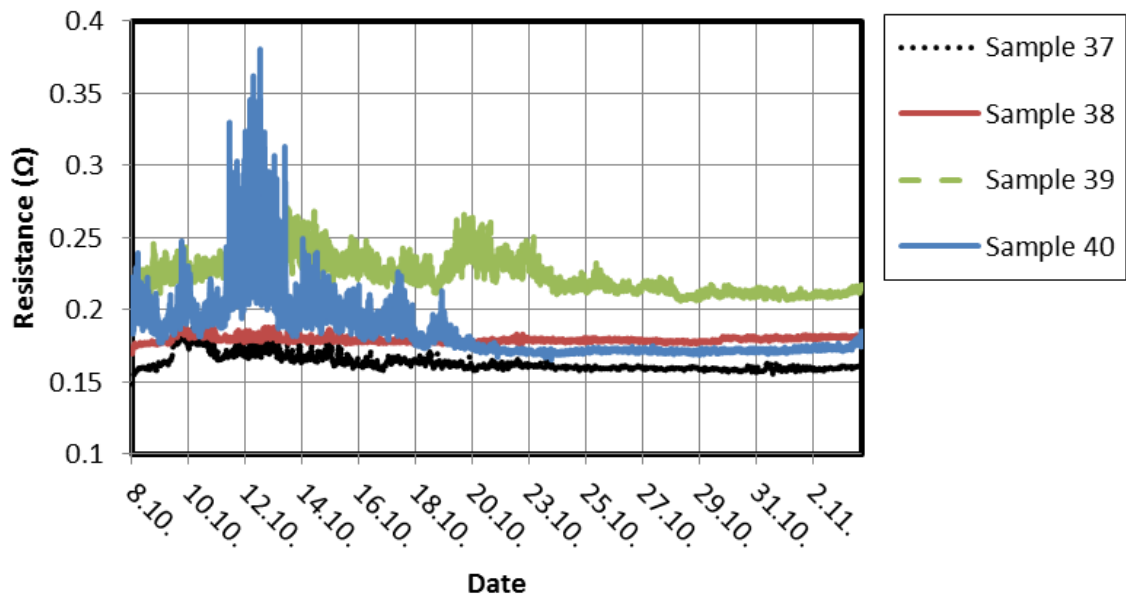


Figure 37. The resistance changes of plated through hole test patterns with conformal coating. No clear change could be achieved during testing

### 6.2.1 Quad flat packages

Quad flat package (QFP) components were chosen in the test to the effect of the high package density to corrosion based short circuit failures. As can be seen from figure 38, the uncoated QFPs lose approximately 10 % of their original insulation resistances but do not go into a short circuit.

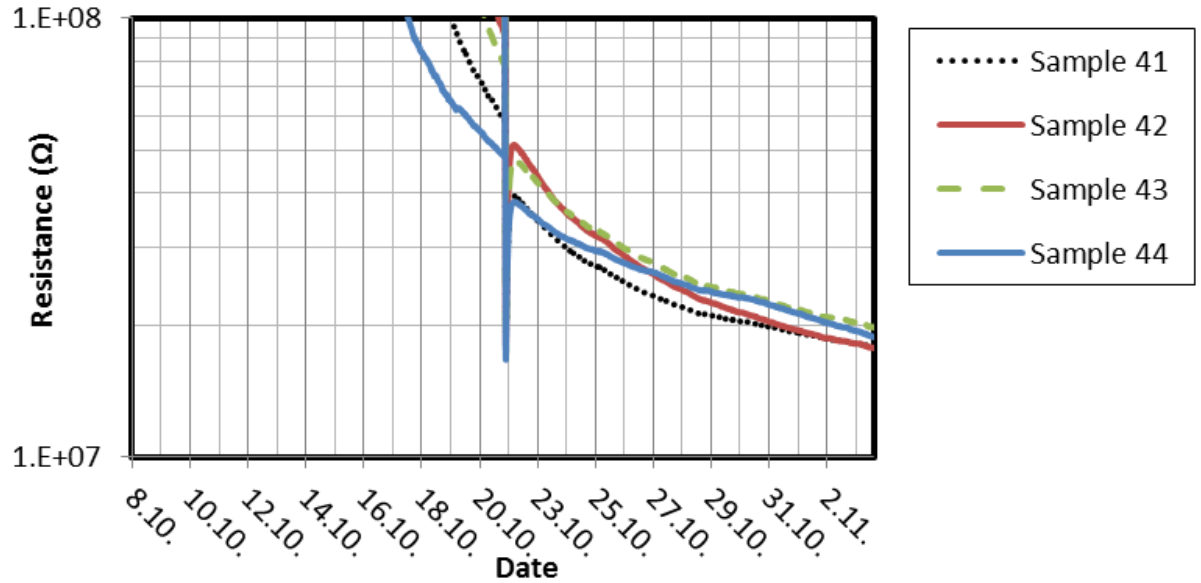


Figure 38. Resistance changes of uncoated quad flat packages. During 28 days test time uncoated QFPs lost almost 10 % of their resistance but they did go into a short circuit. Conformal coated QF-patterns did not show resistance change during testing.

In the case of conformal coated QFPs the surface resistances did not decrease into a measurable range.

### 6.2.2 Serial and parallel resistors

The resistances of serial resistor with or without conformal coating did not show clear change during the four weeks test period. However, in the case of parallel resistors, uncoated samples showed small but not remarkable decline (change less than 1 %) while conformal coated samples did not react at all. Resistances for serial resistors are presented in figures 39 and 40 and parallel resistor in figures 41 and 42.

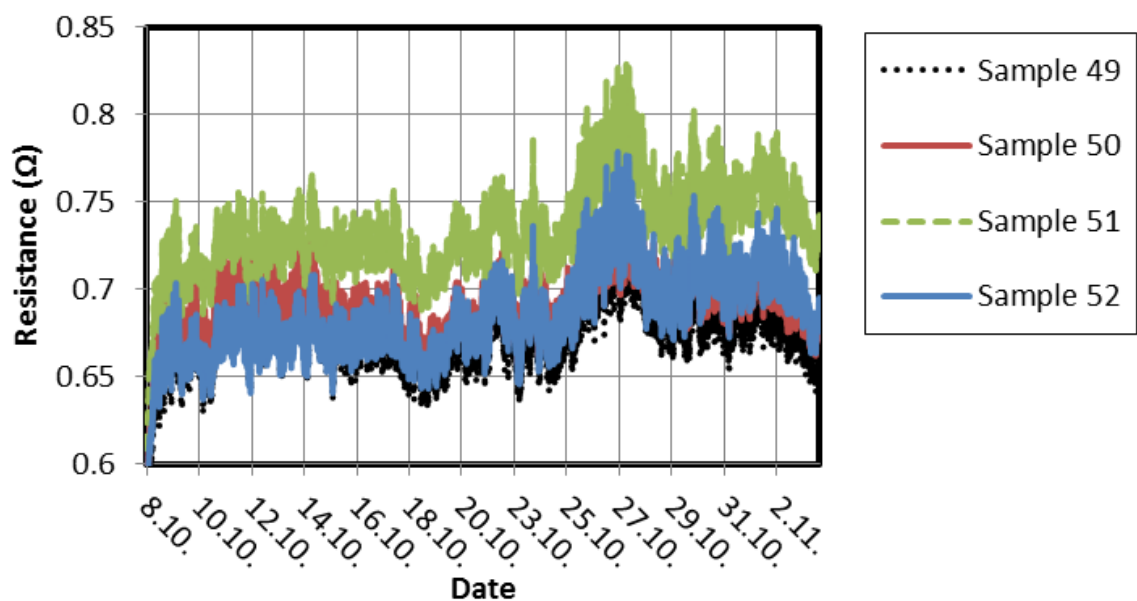


Figure 39. Resistance changes of uncoated serial resistors. No clear resistance change could not be achieved during testing.



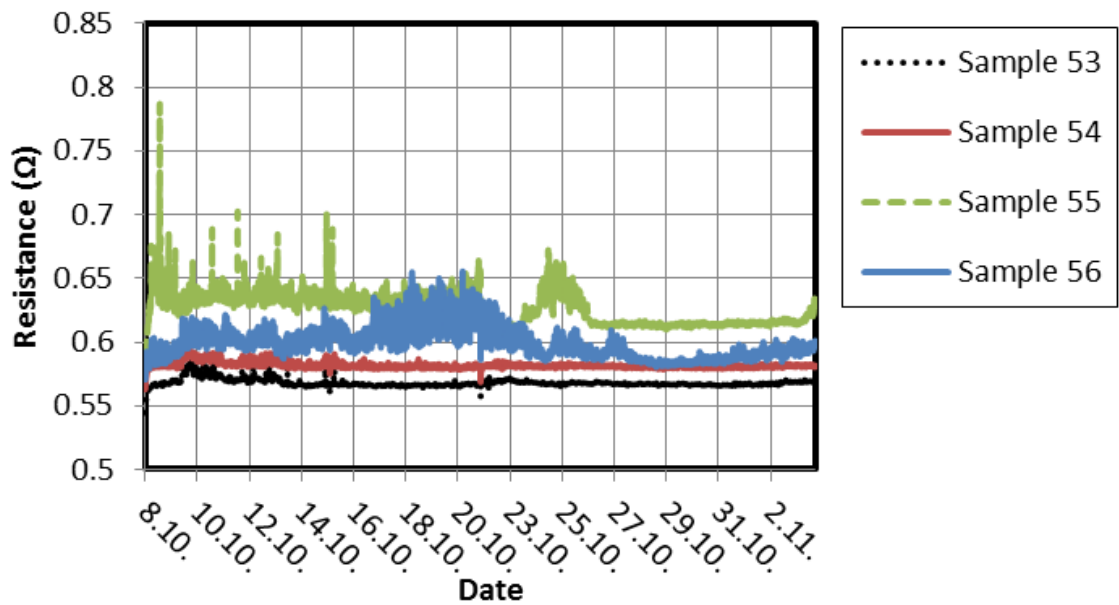


Figure 40. Resistances of conformal coated serial resistors. These resistances did not change during testing.

The resistances of serial resistors are less than  $1\ \Omega$ , which is due to small resistors used in these test patterns. In test patterns of serial and parallel resistors the surface resistances of conformal coated cases are slightly smaller than with uncoated patterns.

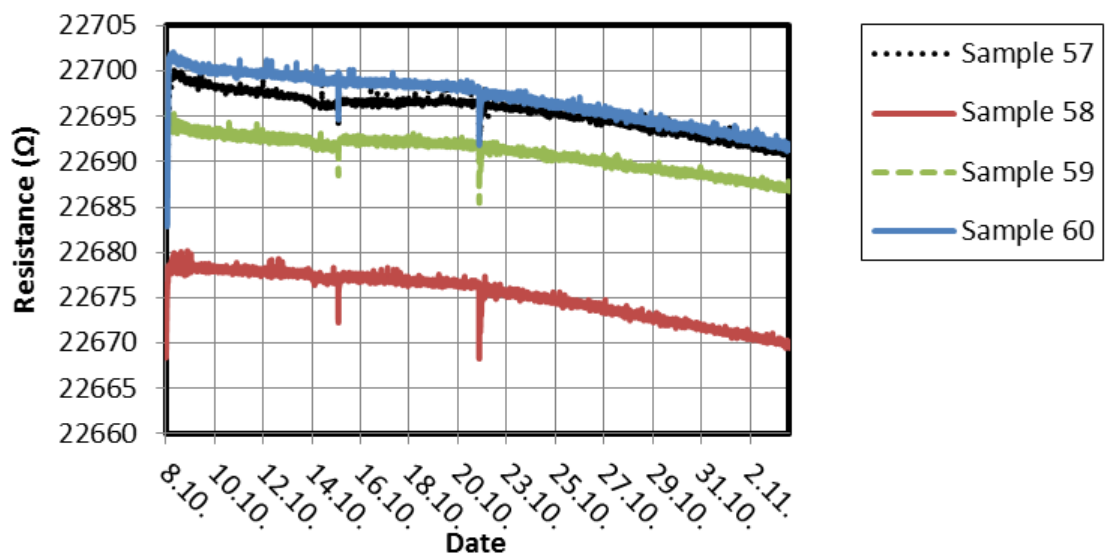


Figure 41. Resistance curves of uncoated parallel resistors. Only small change ( $< 1\%$ ) can be seen in these curves.

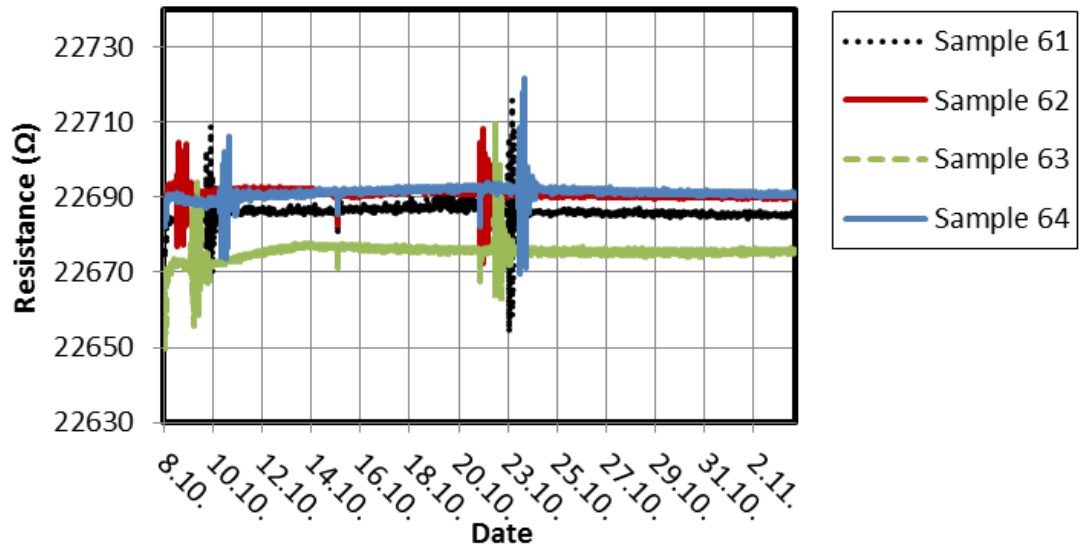


Figure 42. Resistances of conformal coated parallel resistors. No clear change was achieved during testing.

### 6.2.3 Other reference samples

Connectors, plastic liquid-crystal displays (LCD) control panels and PCB plates were tested alongside with sensor and reference component PCB in the corrosion test. They were not connected to data loggers and their corrosion monitoring was carried out by literal inquiry, because these samples were collected by different branches of ABB. Because this corrosion monitoring was done mostly by visual inspection and only part of connectors was tested electronically, functionality results from these samples were deficient. These results are given in table 17. In conductors, base material was usually brass coated with copper as an under coating followed by electroless nickel immersion gold nickel–gold plating (ENIG). In this plating type nickel layer is coated with a thin gold layer. Other material choice for contactors was flash golding or pure nickel. ENIG and hot air solder levelled (HASL) are both used for soldered parts. Plastic part survived well and LCD displays functioned without problems after test. Gold and organic solder ability preverrated copper survived worst and silver and nickel best. It seemed, that thick silver and hard nickel plating could prevent humidity and corrosive gases to penetrate through the passive layers, while soft gold plating were more prone to corrosion.

Table 17. Reference samples plating materials, corrosivity and functionality.

Material/plating	Plating thickness	Corrosivity	Functionality
Immersion nickel	1–10 $\mu\text{m}$	slight	n/a
Immersion silver	30–50 $\mu\text{m}$	slight	ok
Flash gold	0.6–0.8 $\mu\text{m}$	bad	n/a
Nickel–gold plating (ENIG)	1–10 $\mu\text{m}$ nickel followed by 0.3 – 30 $\mu\text{m}$ gold layer	bad	Small problems
Organic solder ability preservative coated copper	n/a	bad	destroyed
Soldered parts (HASL)	n/a	ok	ok

### 6.3 Test corrosiveness on copper

SEM-pictures, Energy-dispersive X-ray spectroscopy (EDS) and copper coupon corrosion results are presented here. EDS is a tool commonly attached to a SEM microscope. This method utilizes x-ray beams which excite its own x-ray radiation. This excited radiation varies according to its source materials and it can be used for elemental analysis or chemical characterization of a sample.

Two samples used for SEM-imaging and EDS analysis are presented in figure 43. The cross-section area is presented with red lines. The thinner part was used for SEM-picture and the larger pieces were used for EDS analysis.

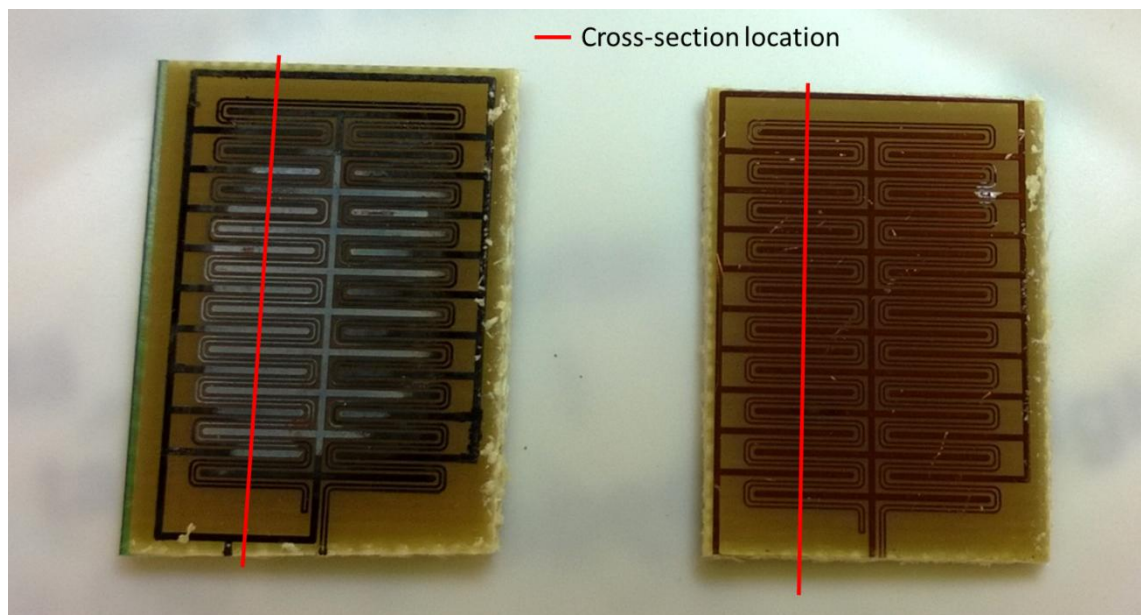


Figure 43. Corrosiometer samples for SEM-analysis. The corrosiometer in the left is a gas-tested bare copper sensor and the right one is an untested bare copper sensor. The cross-section area is presented with red lines and larger sample part was used for SEM-imaging and the smaller one for EDS-analysis.

The sample in the left is the gas-tested sample and the right one is the un-tested-reference sample. According to EDS-analysis the black area is copper oxide and the white area is mixture of copper chloride and copper sulphide with copper oxide underneath.

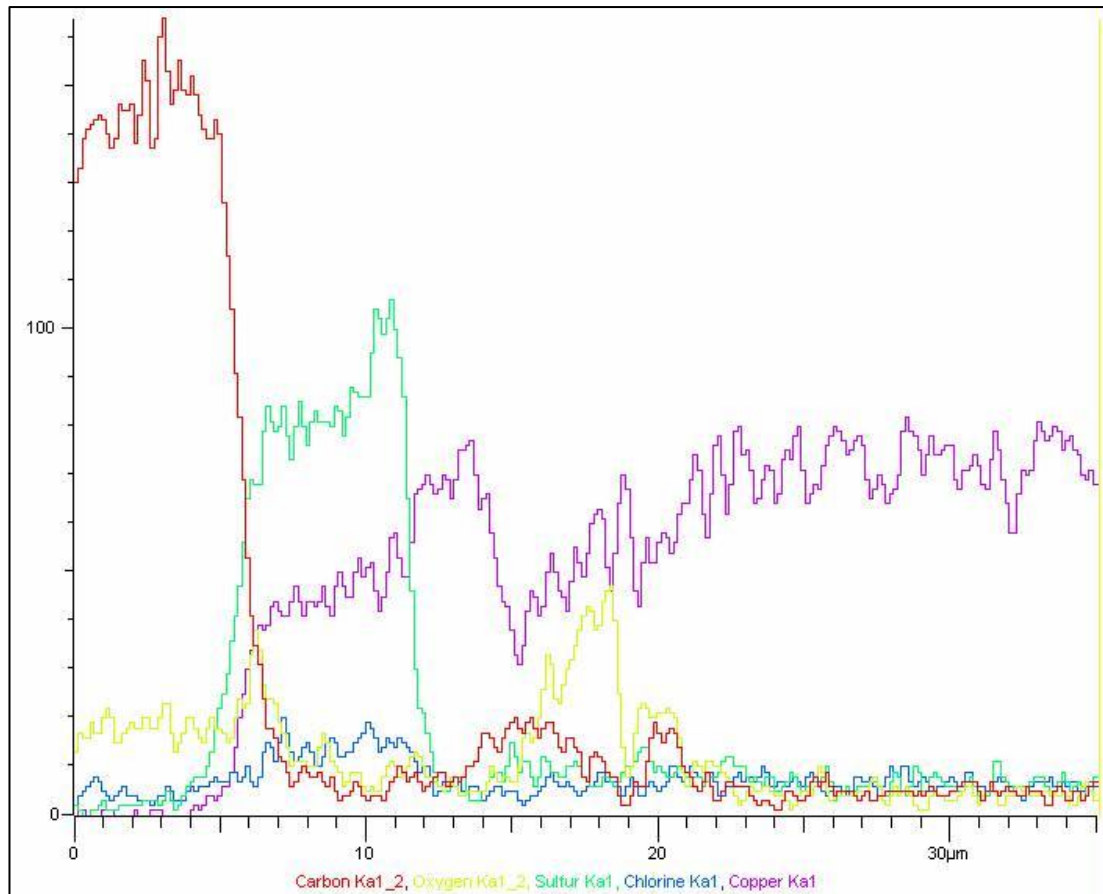


Figure 44. An EDS-analysis example from the gas-tested sample. The analysis graph shows excitation radiation energy vs. the depth from the surface of the material. According this analysis there is a notable source of C on top the sample (red line) which is probably caused by FR-4 base material, which contains hydrocarbons. Purple line presents for Cu. On top of the sample there is layer which contains S (green line) and Cl (blue line) which form a mixed compound with copper. Beneath this mixed layer there is CuO (yellow line for oxide).

Figures 45 and 46 give the dimensions from the cross section of a copper trace. In figure 45 the double surface layer is clearly visible. Based on these SEM pictures, following can be said. The depletion of the copper layer was approximately 5 μm, which is more than the expected 1.4 μm. However, as can be seen from figures 45 and 47, a majority of copper trace has not corroded, which means that a great deal of the sensor's use life is still un-used. Thickness of the corrosion product layer was approximately 10 μm. This corrosion product layer is brittle and fragmented.

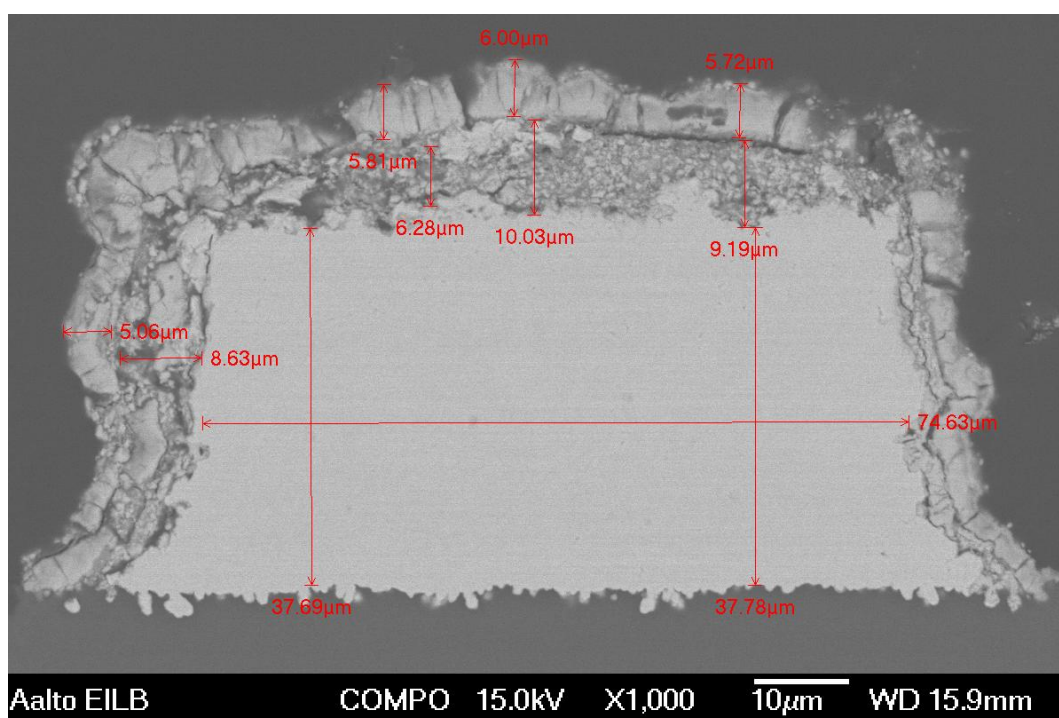


Figure 45. A SEM picture from the gas tested sample with dimensions. On top there is a scaling and brittle copper-sulphur-chlorine mixed layer whose thickness is approximately 5  $\mu\text{m}$  followed by copper-oxide layer with same thickness. Beneath these layers denser unreacted copper can be found.

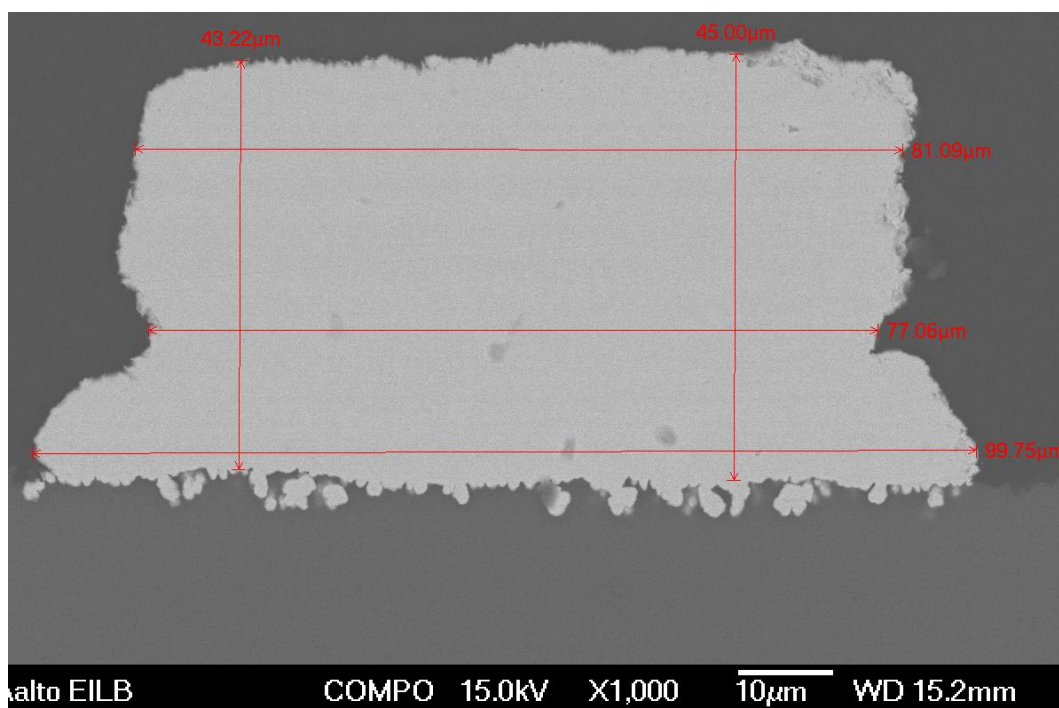


Figure 46. A SEM picture from the reference sample with dimensions.

Samples were also imaged with an optical microscope. In figure 47 two optical microscope pictures are presented together. The red area is un-corroded copper and the grey area corroded copper.



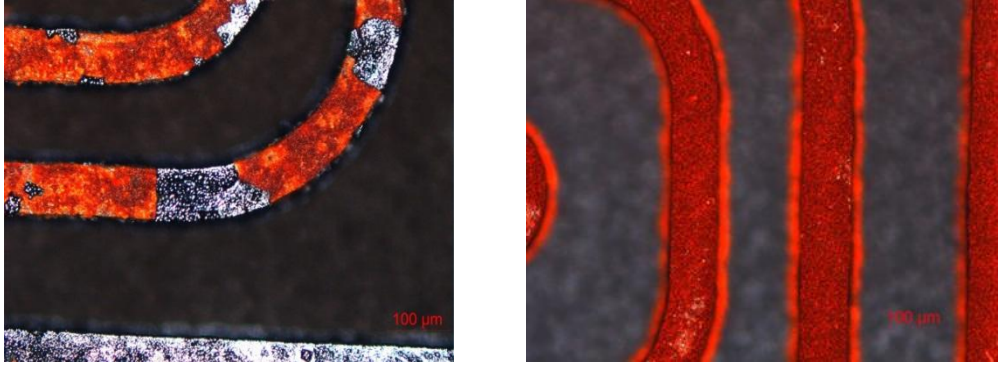


Figure 47. Optical microscope figures from the copper traces on the samples. Red areas are unreacted copper and black areas are copper-oxide.

In a table 18, the theoretical conductor resistance and its change, due to 5 µm corrosion depth of copper, are calculated between the tested and untested sample in temperatures 20 and 30 °C.

Table 18. Resistances in gas-tested and untested reference sample in temperatures 20 and 30 °C.

Sample	Length (m)	Thickness (µm)	Width (µm)	Area (mm <sup>2</sup> )	$\rho_{Cu}$ in 20 and 30 °C (Ω*m)	$R_C$ in 20 °C (Ω)	$R_C$ in 30 °C (Ω)
Reference	0.48	45	85	$3.8 \cdot 10^{-8}$	$1.7 \cdot 10^{-8}$	2.1	2.2
Gas-tested	0.48	40	75	$3.6 \cdot 10^{-8}$	$1.8 \cdot 10^{-8}$	2.7	2.8
					$\Delta R_C$	0.6	0.6

#### 6.4 Summary of results and comparison with Vahter's results

Jukka Vahter did corrosion testing with PCB by utilizing 85°C/85% method. Typical surface resistances at beginning of the test were 100–200 MΩ and after 500 h in 85°C/85% test the surface resistances were 300–3000 MΩ. His test pattern made by copper traces was given in figure 17, page 36. Vahter's result graphs are given in appendix C.

Vahter's average surface resistances for bare copper and solder resist coated traces are given in figure C1. Used copper trace widths and spacings were 0.5 and 0.25 mm, 0.5 and 0.5 mm and 0.25 and 0.1 mm and 0.1 and 0.1 mm, which were the closest option the sensor proposed and tested in this Master's Thesis. In Vahter's test set-up the resistance rises from 200 MΩ to over 3000 MΩ. This is the opposite behavior to the bare copper insulator resistance curves given in figure 34, where the resistances were beyond measurable range at first and then lowers into 100–1000 MΩ. It is difficult to say how much of this behavior is due to the fact that behavior of the insulator resistance at the beginning of test is unknown due to improper measurement range and how much is the result of different measurement techniques and sample construction and.

For better understanding also all the curves for 0.1 mm spacing and trace widths are presented in figure C2. It can be seen that the surface resistances for bare copper traces are much higher than with older resist coated cases. Again the data from insulation resistance is fragmented, as the resistance values exceed the scale, and these data curves are typically higher than the bare copper insulation resistances.

Zhan, Azarian and Pecht (2006) examined how high temperature and humidity affects to the surface insulation resistance in IPC-B-25 test coupons. These boards each consisted of three comb structures, with to 0.16, 0.32, and 0.64 mm (marked as In order to investigate leakage current and dendritic growth between solder joints, the comb structures were coated with a eutectic (63 Sn/37 Pb) solder.

They used two different test set-ups (with 168 hours test time for each test) which were

- 85 °C/85 % RH and
- 40 °C/90 % RH.

According to their results, the starting value for all test coupons were  $2 \times 10^{12} \Omega$ . After 85 °C/85 % RH testing all surface insulation resistance values were  $10^9$ – $10^{10} \Omega$  with no values below  $2 \times 10^9 \Omega$ , so no short-cuts occurred. They suspected that the high temperature allows the plating material to dissolve and to form a well conductive electrolyte together with condensated water. In the latter test set-up, lower resistance value were achieved and their values are given in figure C3, which can be found from appendix C.

As Zhan, Azarian and Pecht (2006) noted, only comb structures with 0.32 mm spacing failed instead of smallest 0.16 spacing which would have been more likely to happen. Failure analysis of the PCB surface showed that only 0.32 mm comb structure had organic fiber contamination. These fibers were born prior to conformal coating either during or after application of the flux. Because a goal for Zhan, Azarian and Pecht research was to inspect flux residues, no cleaning was carried out before conformal coating in order to avoid removing any residues.

## 7 Conclusions

The proposed corrosiometer is applicable for corrosion monitoring. It can be seen that the bare copper test pattern reacts linearly during four weeks tests time. From the SEM pictures it can be deduced that the Telcordia outdoor corrosion test took just a fraction of the sensors life-time. For linear signal a reference pattern must be used which can be either pattern coated with solder resist, immersion tin or conformal coating.

Mixed flow corrosion tests are good for corrosion monitoring from low to moderate corrosion atmospheres (C1–C4 in ISO 9223 categorization) and for extreme environments such as seashore and seawater salt spray tests combined with gas tests are more applicable. However, in these harsh test set-ups, PCBA must be tested with proper encapsulation because bare PCBAs will be destroyed in a manner which does not simulate accurately field environments.

This Master's Thesis gives a model for a corrosiometer which can be manufactured by using same materials and processes as the PCBs and therefore it is as good as any PCB it monitors. The equipment for corrosiometer signal measurement and processing was left out from this Master's Thesis. Also field tests are needed if this sensor is going to be used to monitor drives in different environments.

For future research, it would be beneficial to compare the sensor presented in this Master's Thesis with field tests, perhaps as a member of a larger conditions monitoring system. This monitoring system could include humidity and temperature sensor, which would give relevant information of how temperature and humidity changes affect the corrosiometer's resistance. It would be important if the data collected by this condition monitoring system is needed in life cycle estimations. It would also be beneficial to monitor mechanical shaking or shocks with accelerometer or gyroscope because failures are usually caused by both mechanical and chemical over-load.

If these sensors are going to be used to use in very corrosive environments, such as sea-side or marine condition, encapsulated corrosiometers should first be tested with 85 °C/85 % RH or 40 °C/90 % RH, salt sprays or flowing mixed gas tests combined salt sprays (for example ISO 21207).



## References

- ABB Oy. 2013a. ABB machinery drives ACS355 0.37 to 22 kW/0.5 to 30 hp Catalog. 23 P.
- ABB Oy. 2013b. ABB industrial drives ACS880, multidrives 1.5 to 250 kW Catalog. 27 P.
- Aromaa, J. 2005. Korroosionestotekniikan perusteet. Espoo, Finland: Helsinki University of Technology. P. 132. ISBN 951-22-7829-4.
- Chen, W. 2000. Determining Dielectric Constant and Loss Tangent in FR-4. UMR EMC Laboratory Technical Report: TR00-1-041.
- Comizzoli R., Franey J., Graedel T., Kammlott G., Miller A., Muller A., Peins G., Psota-Kelty L., Sinclair J. and Wetzel R. 1992. The Kuwait Environment and its Effect on Electronic Materials and Components. Journal of the Electrochemical Society. Vol. 139:7. P. 2058–2066. DOI: 10.1149/1.2221175. ISSN 0013-4651.
- GR-63-CORE. 2002. NEBS Telcordia Outdoor standard. 158 P.
- Hæggström, E, Paulin, T. and Holmström A. 2013. Malliratkaisut 3, Fysiikan mittausmenetelmät I-course material. University of Helsinki, department of Material Physics.
- Henriksen, J., Hienonen R., Imrell, T., Leygraf, C. and Sjögren L. 1991. Corrosion of Electronics: Handbook based on Experiences from Nordic Research project. Stockholm, Sweden: Korrosionsinstitutet. 86 P. ISBN: 91-87400-02-2.
- Hienonen, R. and Lahtinen, R. 2007. Corrosion and climatic effects in electronics. Espoo, Finland: VTT publications. 415 P. ISBN 978-951-38-6992-2
- IEC 60721-3-3. 1994. Classification of environmental conditions. Part 3: Classification of groups of environmental parameters and their severities. Section 3: Stationary use at weather protected locations. 100 P.
- IPC-TM-650 Test Methods Manual. 2013. Tests methods 2.6.3.3, 2.6.3.4 and 2.6.3.6. [Cited 23.01.2014]. Available: <https://www.ipc.org/ContentPage.aspx?pageid=Test-Methods>
- ISO Organization. 2012. ISO 9223. Corrosion of metals and alloys. Classification of corrosivity of atmospheres. 15 P.
- ISO 10062. 2006. Corrosion tests in artificial atmosphere at very low concentrations of polluting gases. P. 12.
- Karppinen, J. 2013. Reliability assessment of electronic assemblies under multiple interacting loading conditions. Doctor dissertation. Aalto University, School of Electrical Engineering, Department of Electronics. Espoo, Finland. 78 P. ISBN: 978-952-60-4995-3

Kiiski, T. 2012. Taajuusmuuttajien luotettavuus, huollettavuus ja kunnossapito teollisessa ympäristössä. Master's Thesis. Tampere University of Technology, Program in Electrical Engineering. Tampere, Finland. 73 P.

Niemi, M. 2006. Nopea sarjatuotoinen linkki taajuusmuuttajan sisäisessä tiedonsiirrossa. Master's Thesis. Helsinki University of Technology, Department of Electrical and Communications Engineering. 78 P.

Niiranen, J. 2000. Sähkömoottorikäytön digitaalinen ohjaus. Helsinki, Finland: Otatieto Press. Second Edition. 381 P. ISBN: 951-672-300-4.

Prosek, T. 2006. Automated corrosion sensors for on-line real time monitoring of indoor and outdoor atmospheres. Proc. of 7th Indoor Air Quality Meeting Braunschweig, Germany, November 15–17, 2006.

Ready W. and Turbini L. 2000. A Comparison of Hourly Versus Daily Testing Methods for Evaluating the Reliability of Water Soluble Fluxes. IEEE Transactions on advanced packaging, Vol. 23:2, P. 285–292.

Revie W. 2000. Uhlig's Corrosion Handbook. Chapter 18, Atmospheric Corrosion. P. 205–322. 1228 P. ISBN 0-471-15777-57

Tolvanen, J. 1996. Protection of frequency converter PCBs from corrosion. Master's Thesis. Helsinki University of Technology, faculty of Electrical and Telecommunications Engineering. 68 P.

US 5338432 A. 1994. Corrosivity sensor. Agarwala, W. and Pearlstein F. 87237. 30.06.1993. Published 16.08.1994. 7 P.

US 6564620 B1. 2003. Visually indicating corrosion sensing. Jaeger, P. 29.06.1998. Published 29.06.1999. 11 P.

US 7755501 B2. 2010. Environmental fuse. ABB Oy. Helsinki. Silvennoinen, M. 28.01.2005. 13.07.2010. 17 P.

Vahter, J. Elektroniikkatuotteiden korroosioherkkyyden määrittäminen. 1999. Master's Thesis. Tampere University of Technology, department of Applied Materials Science. P. 67.

Zhan S., Azarian M. and Pecht M. 2006. Surface Insulation Resistance of Conformally Coated Printed Circuit Boards Processed With No-Clean Flux. IEEE Transactions on advanced packaging manufacturing, Vol. 23:2, P. 217–223.

Zhao, P. 2005. Creep corrosion over plastic encapsulated microcircuit packages with noble metal pre-plated lead frames. Doctor dissertation. University of Maryland, Collegepark: USA. 130 P.

## Appendix A. Corrosion rates and corrosion studies in tropical environments

To calculate corrosion rate of copper in field conditions, following results were found from literature.

Southwell, Hummer and Alexander 1966 presented corrosivity results of a 16 year field test in tropical atmosphere and marine coastal zone. Their test materials were copper and copper alloys. Although report is almost 50 year old, it is a valuable because it involves corrosion study in the field without using acceleration tests. According to them, corrosion rates can be calculated by formula 9. Their results are presented in figure A1, which gives corrosion for copper and copper alloys for coastal and inland atmosphere.

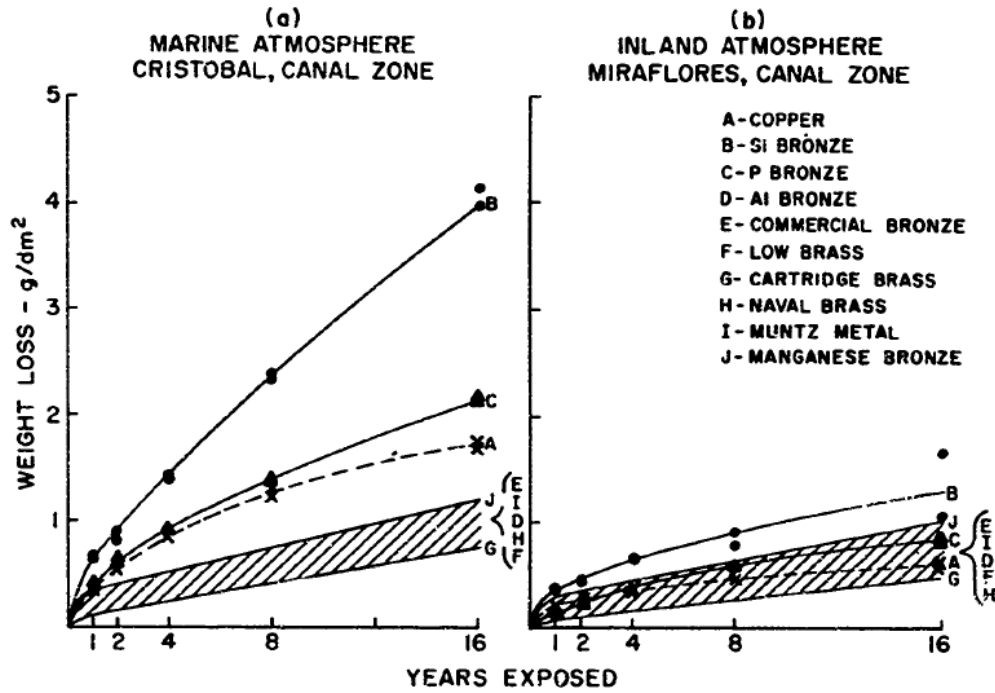


Figure A.1. Corrosion rates of different copper alloys in marine and inland atmospheres (Southwell, Hummer and Alexander 1966)

From these graphs it can be seen that the annual copper corrosion rate for coastal and inland areas were approximately 2 and 1.5 g/dm<sup>2</sup>. These can be changed into annual copper deposition rates by dividing this corrosion rate with copper density (as in formula 9), which is 8960 kg/m<sup>3</sup> and test time (16 years).

By this calculation coastal copper deposition rate is

$$\begin{aligned}
 2 \frac{g}{dm^2} * \frac{1}{16 \text{ years}} &= 200 \frac{g}{m^2} * \frac{1}{16 \text{ years}} = 12.5 \frac{g}{m^2 * year} * \left(8.96 \frac{kg}{m^3}\right)^{-1} \\
 &= 1.3950 \dots \frac{\mu m}{year} = 1.4 \frac{\mu m}{year}.
 \end{aligned} \tag{A1}$$

For inland copper deposition rate is

$$1.5 \frac{g}{dm^2} * \frac{1}{16 \text{ years}} = 1.5 \frac{g}{m^2} * \frac{1}{16 \text{ years}}$$

$$= 9.375 \frac{g}{m^2 * year} * \left(8.96 \frac{kg}{m^3}\right)^{-1} = 1.046 \dots \frac{\mu m}{year} = 1.0 \frac{\mu m}{year}. \quad (A2)$$

Veleva and Maldonado (1998) have inspected corrosion rates in field tests in Mexico in two annual test periods in 1994 and 1995. Their test places had annual average relative humidity of 75–80 % and temperature near 30 °C. According to their results the corrosivity of all test places were C4–C5 and corrosion rate varied between 32–150 g/m<sup>2</sup>. Again, by dividing these values with copper density, annual copper corrosion could be calculated and they varied between 3.6–17 μm/a.

*Table A.1. Contamination and corrosivity classes according to ISO 9223 and copper corrosion rates (Veleva and Maldonado 1998).*

Test place	Cl-contamination class ISO 9223	SO2 Contamination class ISO 9223	Corrosion class ISO 9223	Annul Copper corrosion rate (g/m2)	Annul Copper corrosion rate (μm/a)
Merida	S1	P0	C4	32	3.6
Majahual	S3	P0	C5	93	10
Puerto Morelos	S2–S3	P0	C5	100	11
Progreso	S3	P1	> C5	150	17

## Appendix A References

Southwell, C., Hummer, W. and Alexander A. 1966. Corrosion of Metals in Tropical Environments. US Naval research facility, NRL report 6452. P. 26

Veleva L. and Maldonado L. 1998. Classification of atmospheric corrosivity in humid tropical climates. British Corrosion Journal. Vol. 33:1. P. 53-57. DOI:10.1179/000705998798483517 ISSN 0007-0599

## Appendix B. Sample numbers

In table B.1 sample numbers, material combinations, and knowledge whether they measure conductor resistance ( $R_C$ ) or insulation resistance ( $R_I$ ) are given.

*Table 1.B. Sample numbers*

Sensor patterns			
Bare copper ( $R_C$ )	Bare copper ( $R_I$ )	Solder resist ( $R_C$ )	Solder resist ( $R_I$ )
Sample 1	Sample 5	Sample 9	Sample 13
Sample 2	Sample 6	Sample 10	Sample 14
Sample 3	Sample 7	Sample 11	Sample 15
Sample 4	Sample 8	Sample 12	Sample 16
Immersion tin ( $R_C$ )	Immersion tin ( $R_I$ )	Conformal coating ( $R_C$ )	Conformal coating ( $R_I$ )
Sample 17	Sample 21	Sample 25	Sample 29
Sample 18	Sample 22	Sample 26	Sample 30
Sample 19	Sample 23	Sample 27	Sample 31
Sample 20	Sample 24	Sample 28	Sample 32
Component patterns			
Uncoated PTHs	Conformal Coated PTHs	Uncoated QFPs	Conformal Coated QFPs
Sample 33	Sample 37	Sample 41	Sample 45
Sample 34	Sample 38	Sample 42	Sample 46
Sample 35	Sample 39	Sample 43	Sample 47
Sample 36	Sample 40	Sample 44	Sample 48
Uncoated PTHs	Conformal Coated PTHs	Uncoated QFPs	Conformal Coated QFPs
Sample 49	Sample 53	Sample 57	Sample 61
Sample 50	Sample 54	Sample 58	Sample 62
Sample 51	Sample 55	Sample 59	Sample 63
Sample 52	Sample 56	Sample 60	Sample 64

## Appendix C. Reference result graphs for chapter 6.4

Figure C1 and C2 are Surface resistance changes presented in Vahter Master`s Thesis. Vahter used 85 °C/85 % RH test for this research. Figure C1 gives average surface insulation resistance with bare copper and with solder resist coated copper traces. The used sensor pattern is given in figure 18. Used copper trace widths and spacings were 0.5 and 0.25 mm, 0.1 and 0.1 mm, 0.5 and 0.5 mm and 0.25 and 0.1 mm.

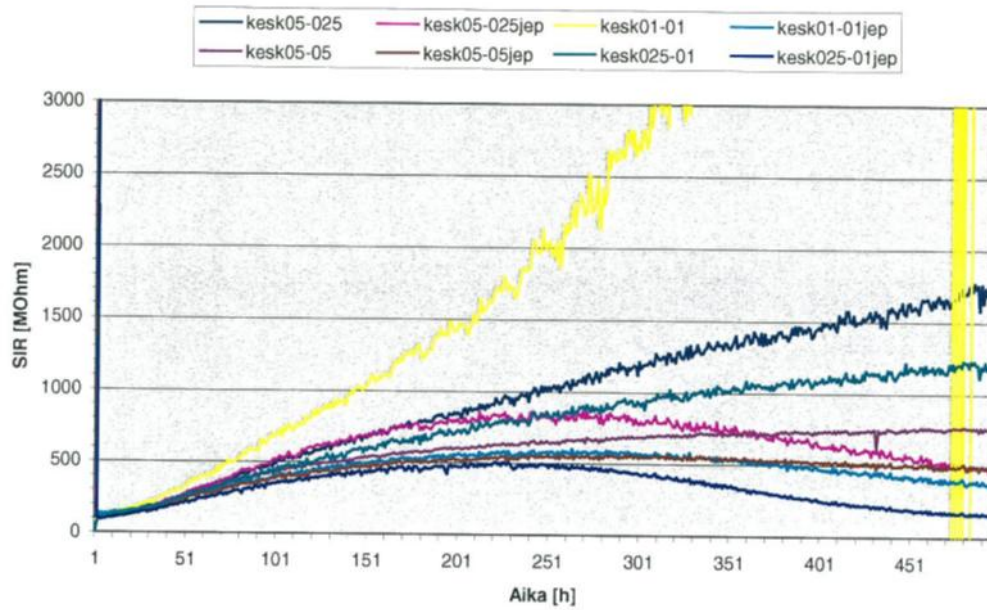


*Figure C1. Average surface resistances for bare copper traces vs. traces coated with solder resist which were tested by sensor structure given in figure 18. Used copper trace widths and spacings were 0.5 and 0.25 mm, 0.5 and 0.5 mm and 0.1 and 0.1 mm.*

Figure C2 gives surface resistances for copper traces with 0.1 mm spacing and trace widths.

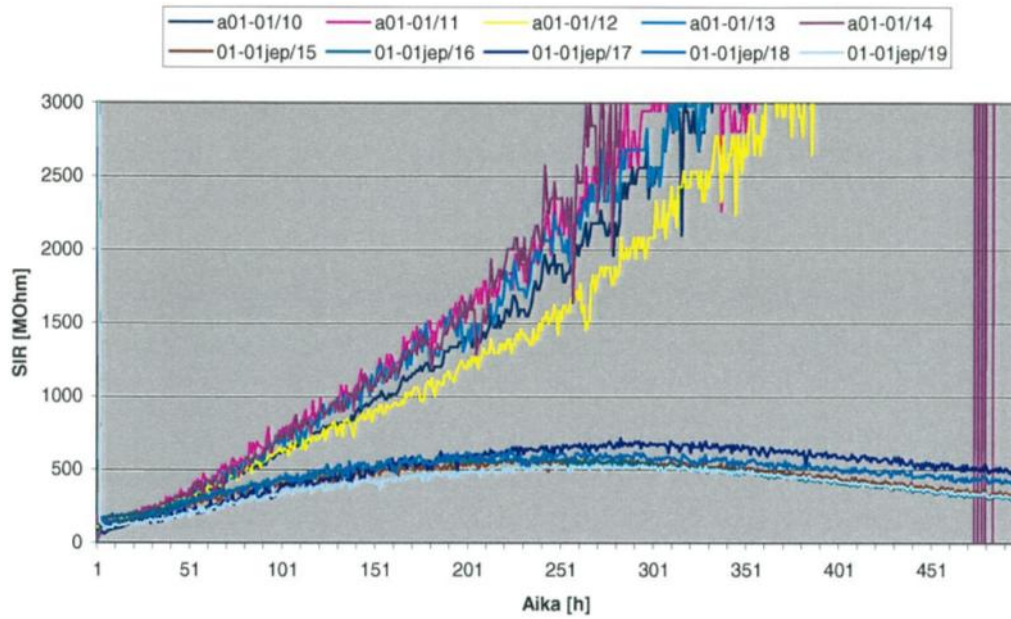


Figure C2. Surface resistances for copper traces with 0.1 mm spacing and trace widths (Vahter 1999, P. 75).

Zhan, Azarian and Pecht (2006) measured Surface Insulation resistance with 40 °C/90 % RH. Their results are given in figure C3.

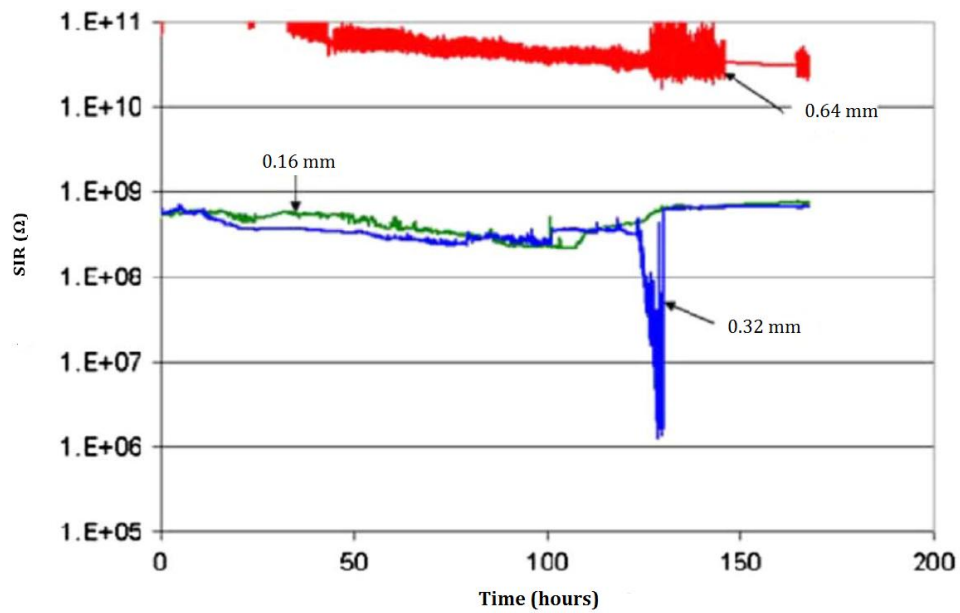


Figure C3. Surface resistance values for 40 °C/90 % RH test set-up values.